Universidade de Aveiro Departamento de Química

2014

Filipa Alexandra André Vicente

Novos sistemas micelares de duas fases aquosas com líquidos iónicos

Novel aqueous micellar two-phase systems with ionic liquids

Universidade de Aveiro Departamento de Química
2014

Filipa Alexandra André Vicente

Novos sistemas micelares de duas fases aquosas com líquidos iónicos

Novel aqueous micellar two-phase systems with ionic liquids

Dissertação apresentada à Universidade de Aveiro para cumprimento dos requisitos necessários à obtenção do grau de Mestre em Bioquímica Clínica. Trabalho realizado sob a orientação científica do Professor Dr. João Manuel da Costa Araújo Pereira Coutinho, Professor Catedrático do Departamento de Química da Universidade de Aveiro, do Professor Dr. Adalberto Pessoa-Jr, Professor Dr., Tilular e Vice-Diretor da Faculdade de Ciências Farmacêuticas da Universidade de São Paulo e co-orientação da Dra. Sónia Patrícia Marques Ventura, Estagiária de Pós – Doutoramento da Universidade de Aveiro.

Aos meus pais e irmão, porque tudo é possível e nada é impossível…

o júri

presidente Prof. Dr. Pedro Miguel Dimas Neves Domingues

professor auxiliar do Departamento de Química da Universidade de Aveiro

Prof. Dr. João Manuel da Costa Araújo Pereira Coutinho

professor catedrático do Departamento de Química da Universidade de Aveiro

Doutora Ana Paula Moura Tavares

investigadora do LSRE da Faculdade de Engenharia da Universidade do Porto

Agradecimentos

Em primeiro lugar quero agradecer ao Professor João Coutinho e ao Professor Adalberto Pessoa Jr. Ao Prof. João quero agradecer por ter aceite orientar-me uma vez mais, por me deixar pertencer ao fantástico grupo que é o PATh e por me ter permitido realizar esta tese em colaboração com a Faculdade de Ciências Farmacêuticas da Universidade de São Paulo. Ao Prof. Adalberto tenho de agradecer por me ter recebido tão bem e por estar sempre disposto a tirar-me dúvidas.

Os próximos agradecimentos são dirigidos aos meus pais e irmão, pois eles foram sem dúvida alguma os meus pilares e o meu porto seguro durante este ano conturbado e difícil, especialmente a minha mãe, que é a luz na minha vida, mais que uma mãe é uma melhor amiga!

Um obrigado muito especial à minha família por todo o apoio, todo o carinho e toda a dedicação que me ajudou a ultrapassar alguns meses complicados no Brasil.

Quero agradecer aos meus melhores amigos, Daniela e Fábio, que mesmo com um oceano no meio, continuaram a ser duas das pessoas imprescindíveis na minha vida e nunca mudaram!

Ao João, um sincero obrigado por ter sido o amigo que foi e por termos partilhado todos aqueles momentos de alegria, risada, aventuras, mas também de tristeza, susto e sofrimento ao longo dos nossos meses no Brasil.

À Sónia fica um agradecimento muito especial porque mais que uma orientadora tem sido uma excelente amiga! É uma pessoa incansável que me apoia e ajuda não só na minha vida profissional mas também na minha vida pessoal. Obrigado por tudo!

Não posso deixar de agradecer também a um bom amigo e ex-orientador, o Jorge, por me ter ensinado todas as bases que precisava para ser uma boa investigadora, estas foram imprescindíveis na minha estadia no Brasil! Obrigado por seres o amigo que és e por seres um mentor profissional e me guiares num bom caminho desde que nos conhecemos!

Um muito obrigado à Luciana Pellegrini e à Luciana Lário por toda a amizade, todo o carinho e apoio, e por tudo o me ensinaram ao longo dos meus meses na USP.

Ao André e à Sabrina devo um enorme obrigado por me terem adotado como a filhota portuguesa, por terem sido uns excelentes amigos e me terem ensinado tanto.

A todos os elementos do LabBioTec e do Path um muito obrigado pela amizade, carinho e ajuda, em especial à Francisca que me tem acompanhado e ensinado tanto nestes últimos tempos.

Palavras-chave

Sistema micelar de duas fases aquosas, Triton X-114, líquido iónico, co-surfactante, extração seletiva, tecnologia de extração, técnica analítica

Resumo

Este trabalho visa o desenvolvimento de novos sistemas micelares de duas fases aquosas (SMDFA) usando líquidos iónicos (LIs) como co-surfactantes e a avaliação da sua capacidade extractiva para várias (bio)moléculas. Numa primeira abordagem, foram determinadas as curvas binodais, usando o Triton X-114 como surfactante e LIs pertencentes às famílias imidazólio, fosfónio e amónio quaternário. Deste modo, foi possível estudar o efeito da ausência/presença de vários LIs, bem como da sua concentração e componentes estruturais, no comportamento das curvas binodais. Posteriormente, os SMDFA foram aplicados em estudos de partição pela utilização de duas moléculas modelo, a proteína citocromo c e o corante rodamina 6G. Verificou-se que a presença de LIs como co-surfactantes aumenta não só os coeficientes de partição, mas também a seletividade do processo extrativo.

Os novos SMDFA foram aplicados à extração do corante natural curcumina, a partir do extrato vegetal com recuperação completa na fase rica em micelas, embora existam interações ainda desconhecidas a afetar a estrutura da curcumina.

Por fim, os SMDFA desenvolvidos foram propostos como métodos alternativos para o pré-tratamento de amostras, no contexto da química analítica. Estes foram usados na reconcentração do antiretroviral tenofovir disoproxil fumarato na fase orgânica, permitindo a sua posterior quantificação e análise. Após otimização das condições operacionais, os resultados obtidos mostraram eficiências de extracção de 100%.

Keywords Aqueous micellar two-phase systems, surfactant, Triton X-114, ionic liquids, selective extraction, curcumin, tenofovir

Abstract

This work addresses the design of novel aqueous micellar two-phase systems (AMTPS) using ionic liquids (ILs) as a new class of co-surfactants for extractive processes and the assessment of their potential of application to the extraction of diverse (bio)molecules. Firstly, the coexistence curves of AMTPS based on the surfactant Triton X-114 and distinct ILs composed of imidazolium, phosphonium and quaternary ammonium structures were determined. These allowed the investigation of the impact of IL absence/presence, concentration and structural features on the behavior of the coexistence curves. The designed AMTPS were then used to carry out partition studies involving two model (bio)molecules, the protein Cytochrome c and the dye Rhodamine 6G. It was shown that the presence of ILs as co-surfactants is able to enhance not only the partition coefficients, but also the selectivity parameters of the process.

These AMTPS were also applied to the extraction of the natural colorant curcumin from its vegetal extract with complete recovery into the micelle-rich phase however, there are interactions, yet unknown, affecting curcumin extraction.

Finally, the new AMTPS were proposed as suitable techniques to be used in the domain of analytical chemistry. Hence, they were used in the extraction of tenofovir disoproxil fumarate, an antiretroviral, in order to facilitate its detection. After optimizing several operational parameters, it was possible to attain extraction efficiencies up to 100%. As the current techniques may present low efficiencies and require the use of organic solvents, AMTPS are envisaged as more sustainable approaches.

Contents

LIST OF TABLES

LIST OF FIGURES

■, log $K_{Cyt\ c}$ at 0.3 wt% IL; ■, log $K_{Cyt\ c}$ at 0.5 wt% of IL; ■, log K_{R6G} at 0.3 wt% IL; ■, log K_{R6G} at 0.5 wt% of IL.

Figure 8. Selectivity results obtained through the application of all AMTPS studied for the extraction of R6G and Cyt c: ■, 0.3 wt% of IL; ■, 0.5 wt% of IL.

Figure 9. Illustration of the partition of Cyt c and R6G by applying the AMTPS developed in separate systems and at the same extraction systems, in a clear evidence of the selective character of this liquid-liquid extraction methodology.

Figure 10. Chemical structure representation of the chemicals studied **a)** the cations and anions composing the ILs and **b)** curcumin.

Figure 11. Stability tests of the oleoresin extract considering the colorant concentration - CC (%) - that remains after exposure to different conditions tested: the presence of only Triton X-114, McIlvaine buffer, each one of the imidazolium-based ILs (0.3 wt% and 0.5 wt%) and the phosphonium-based ILs (0.3 wt%) and then the complete AMTPS: ■, 89.7 wt% McIlvaine buffer; ■, 10 wt% Triton X-114; ◆, 0.3 wt% [C_{10}mim]Cl; ◆, 0.5 wt% [C_{10}mim]Cl; ●, 0.3 wt% [C_{12}mim]Cl; ●, 0.5 wt% [C_{12}mim]Cl; ▲, 0.3 wt% [C_{14}mim]Cl; ▲, 0.5 wt% [C_{14}mim]Cl; ◆, 0.3 wt% [C_{10}mim]Cl + 10 wt% Triton X-114 + 89.7 wt% McIlvaine buffer; ●, 0.3 wt% [$P_{6,6,6,14}$]Cl; ●, 0.3 wt% [$P_{6,6,6,14}$]Cl + 10 wt% Triton X-114 + 89.7 wt% McIlvaine buffer; ✳, 0.3 wt% [$P_{6,6,6,14}$]Br; ✳, 0.3 wt% [$P_{6,6,6,14}$]Br + 10 wt% Triton X-114 + 89.7 wt% McIlvaine buffer; ◆, 0.3 wt% [$P_{6,6,6,14}$]Dec; ◆, 0.3 wt% [$P_{6,6,6,14}$]Dec + 10 wt% Triton X-114 + 89.7 wt% McIlvaine buffer; ▲, 0.3 wt% [$P_{6,6,6,14}$][TMPP]; ▲, 0.3 wt% [$P_{6,6,6,14}$][TMPP] + 10 wt% Triton X-114 + 89.7 wt% McIlvaine buffer.

Figure 12. Macroscopic aspect of the colorant after 24 hours of exposure to **a)** [$P_{6,6,6,14}$]Br and **b)** [$P_{6,6,6,14}$]Cl. These ILs were here used just as examples.

Figure 13. Chemical structure representation of **a)** the surfactant, Triton X-114, **b)** the ILs, [C_{14}mim]Cl and [$P_{6,6,6,14}$]Cl and **c)** the polymer, PEG.

Figure 14. Binodal curves for the studied ILs at 0.3 wt% and pH 10: —, without IL; ◆, [C_{10}mim]Cl; ■, [C_{12}mim]Cl; ▲, [C_{14}mim]Cl; ✳, [$P_{6,6,6,14}$]Br; ●, [$P_{6,6,6,14}$][Dec]; □,

$[P_{6,6,6,14}][TMPP]$; The effect of ILs' structural features is provided separately in the insets to facilitate the analysis.

Figure 15. Effect of the pH on the T_{cloud} for all the studied ILs, at 0.3 wt%. In **a)** is presented the effect on the imidazolium family: —, without IL at pH 7; —, without IL at pH 10; ◆, $[C_{10}mim]Cl$ at pH 7; ◆, $[C_{10}mim]Cl$ at pH 10; ▲, $[C_{12}mim]Cl$ at pH 7; ▲, $[C_{12}mim]Cl$ at pH 10; ●, $[C_{14}mim]Cl$ at pH 7; ●, $[C_{14}mim]Cl$ at pH 10; and in **b)** is presented the effect on the phosphonium family: ✳, $[P_{6,6,6,14}]Br$ at pH 7; ✳, $[P_{6,6,6,14}]Br$ at pH 10; ■, $[P_{6,6,6,14}][Dec]$ at pH 7; ■, $[P_{6,6,6,14}][Dec]$ at pH 10; -, $[P_{6,6,6,14}][TMPP]$ at pH 7; -, $[P_{6,6,6,14}][TMPP]$ at pH 10.

Figure 16. Effect of the fermented broth on the T_{cloud} for the imidazolium family. In **a)** and **b)** it is presented the effect of 0.3% wt and 0.5% wt of IL, respectively : ●, $[C_{10}mim]Cl$ without fermented broth; ●, $[C_{10}mim]Cl$ with fermented broth; ♦, $[C_{12}mim]Cl$ without fermented broth; ♦, $[C_{12}mim]Cl$ m with fermented broth; ■, $[C_{14}mim]Cl$ without fermented broth; ■, $[C_{14}mim]Cl$ with fermented broth.

LIST OF ABBREVIATIONS

AIDS – acquired immunodeficiency syndrome

AMTPS – aqueous micellar two-phase systems

ATPS – aqueous two-phase systems

[C_{10}mim]Cl – 1-decyl-3-methylimidazolium chloride

[C_{12}mim]Cl – 1-dodecyl-3-methylimidazolium chloride

[C_{14}mim]Cl – 1-methyl-3-tetradecylimidazolium chloride

CC – colorant concentration

Cyt c – cytochrome c

CMC – critical micelle concentration

EE_{TDF} – extraction efficiency of tenofovir disoproxil fumarate (%)

FDA – Food and Drug Administration

HIV – human immunodeficiency virus

HPLC – high-performance liquid chromatography

IL – ionic liquid

K – partition coefficient

LDL^- – electronegative low density lipoprotein

LLE – liquid-liquid extraction

Log K – logarithm of the partition coefficient

Log P – logarithm of the octanol/water partition coefficient

LPME – liquid phase microextraction

MS – mass spectrometry

$[N_{8,8,8,8}]Br$ – tetraoctylammonium bromide

$[P_{6,6,6,14}]Cl$ – trihexyltetradecylphosphonium chloride

$[P_{6,6,6,14}]Br$ – trihexyltetradecylphosphonium bromide

$[P_{6,6,6,14}][Dec]$ – trihexyltetradecylphosphonium decanoate

$[P_{6,6,6,14}][N(CN)_2]$ – trihexyltetradecylphosphonium dicyanamide

$[P_{6,6,6,14}][TMPP]$ – trihexyltetradecylphosphonium bis (2,4,4-trimethylpentyl)phosphinate

$[P_{8,8,8,8}]Br$ – tetraoctylphosphonium bromide

PEG 600 – polyethylene glycol with a molecular weight of 600 $g.mol^{-1}$

R6G – rhodamine 6G

R_{Top} – recovery of the molecule towards the top phase

R_{Bot} – recovery of the molecule towards the bottom phase

SAXS – small-angle X-ray scattering

scFV – single chain variable fragment

SPE – solid-phase extraction

SPME – solid phase microectraction

$S_{R6G/Cyt\ c}$ – selectivity of R6G and Cyt c

TDF – tenofovir disoproxil fumarate

WHO – World Health Organization

1. GENERAL INTRODUCTION

1.1. STATE-OF-THE-ART

During the last few years, with the appearance of new biopharmaceuticals and other complex molecules of biotechnological origin, there is a stringent need for improvements at the level of the downstream processing. While several advances in large-scale production methodologies were attained, the downstream processes still remain the main drawback for the scale-up of various processes towards industrial implementation. This is mainly due to technological limitations and the need for multiple unit operations to obtain a final product fulfilling the strict purity and safety requirements (*1*). Downstream processes are divided into two principal classes: the high resolution processes, where chromatographic techniques are included, and the low resolution ones, composed mainly of liquid-liquid extractions (LLE). Chromatographic techniques are the most usual choice in the industrial fields, owing to their simplicity, selectivity and accurate resolution, however such methodologies present some limitations related to their scalability and economic viability and, unless the product is of high value, such as antibodies and antigens, these techniques are represented by the processing of small amounts *per* cycle (*2*). Thus, there is an urgent demand for new separation and purification techniques to be applied in the isolation of biomolecules that present good extractive performances, as well as guarantee the chemical structure and activity of the biomolecule being purified, while maintaining the economic viability of the entire process. LLE has been identified as a suitable technique for downstream processes due to its simple and fast operation. Traditionally, LLE is mostly accomplished by applying environmentally nefarious and expensive organic solvents (*3*). In this context, aqueous two-phase systems (ATPS) emerged as appellative types of LLE, since they are mainly composed of water (65-90%) and do not require the use of organic solvents in the whole process, providing mild operation conditions (*4*, *5*). Additionally, they present a low interfacial tension, great biocompatibility, utilization of cost-effective solvents and ease of scaling-up (*4*, *6*). These systems consist of two aqueous-rich phases of two structurally different compounds that are immiscible in certain conditions of concentration, undergoing phase separation. ATPS are considered highly flexible approaches, since a considerable array of compounds, *e.g.* two polymers (*7*, *8*), two salts (*9*), a salt and a polymer (*10*, *11*) or surfactants, can be used in order to achieve high extraction and purification effectiveness, selectivity and yield (*4*). However, polymeric-based ATPS also display some limitations related with the high

cost of some polymers usually employed, namely dextran, and high viscosities limiting the scale-up. Also, when inorganic salts (often corrosive) are used, some additional requirements regarding the equipment maintenance and the wastewater treatment appear (*12*). Meanwhile, polymeric-based ATPS exhibit a limited range of polarities between the coexisting phases (*13*). In this context, there is an urgent demand for the search of alternative phase forming agents possessing more benign properties from the environmental and procedural points of view.

During the last decade, ionic liquids (ILs) have attracted the attention from both academia and industry in two distinct fields as downstream processes and analytical techniques. This crescent interest relays on their unique properties, such as negligible vapor pressure and lack of flammability – *greener solvents* status – as well as high chemical and thermal stabilities, and low melting points (*14–16*). Moreover, ILs are able to solvate a huge variety of solutes, due to the countless cation/anion possible combinations that can cover a wide range of polarities, describing their character of *designer solvents* (*14*, *15*). Finely tuning their properties, it is possible to develop effective ATPS for a specific application, which is a crucial issue for their application as downstream technologies. In fact, the application of ILs as phase forming agents in ATPS boosts the extractive performance and the selectivity parameters of a wide range of compounds (*14*). The first report on the possibility to form ATPS by adding an imidazolium-based IL and an inorganic salt was presented by Rogers and co-workers (*17*), in 2003. Since then, a massive amount of research has dealt with the study of IL-based ATPS and prompted the publication of a recent critical review (*14*). Accordingly, the main part of the studies is focused on the variation of the structural features of the IL as well as the type of salt employed (*14*). From here, more environmentally friendly routes are created, using either ammonium quaternary and cholinium-based ILs (*18–20*) and citrate-based salts (organic nature) (*18*, *21*). It should be pointed out that nowadays the IL-based ATPS are well beyond the IL-salt combinations, being already reported the use of amino-acids (*22*), carbohydrates (*23*), polymers (*24*, *25*) and even surfactants (*26*, *27*). Nonetheless, when the analytical chemistry field is considered, there are several areas of expertise applying ILs, namely the sample preparation, chromatographic techniques, capillary electrophoresis and finally, as analytical techniques in detection processes (*28*, *29*). The analyte pre-concentration and posterior extraction occurs during sample preparation which is accomplish through LLE or microextraction, in particular the liquid phase microextraction (LPME) or the solid phase microextraction (SPME)

(*28–31*). These techniques have been applied in several types of compounds and processes, for example in the removal of metal ions by LLE (*32–34*) and LPME (*35*); in the extraction of phenolic biomolecules (*36*) accomplished by LLE; in the extraction of polycyclic aromatic hydrocarbons (*37*) using LPME; and in the removal of benzene, toluene, ethylbenzene and o-xylene from water samples with SPME (*38*). Afterwards, the analysis of the extracted analyte is carried out in a separating device, for instance gas chromatography, liquid chromatography and capillary electrophoresis (*28–31*). When ILs are used in gas chromatography stationary phases, they display a dual nature. They are capable of separating both polar and non-polar compounds as if they are representing a polar and non-polar stationary phase, respectively, making them advantageous compared to the commonly stationary phases used (*28, 29*). Moreover, the addition of ILs to the mobile phase of liquid chromatography leads to a decrease in band tailing, reduces the zone broadening and improves resolution (*28, 31*). Since ILs present high conductivity and great miscibility with both water and organic solvents, they have been used in capillary electrophoresis as an easier way to adjust the analyte mobility (*31*).

Aqueous micellar two-phase systems (AMTPS) are specific types of ATPS that use surfactants and appear as promising techniques for bioseparation purposes. This fact is mainly due to their remarkable ability to keep the native conformations and biological activities of the target molecules (*39*), while they are migrating between the coexisting phases. Surfactants are amphiphilic molecules, *i.e.* present a polar, hydrophilic and sometimes charged 'head' and a non-polar hydrophobic 'tail'. When its concentration is above a certain value, *i.e.* the critical micelle concentration (CMC), the surfactant molecules form self-assembling aggregates (*39, 40*). Within micelles, each surfactant molecule displays its 'tail' in the interior, while its 'head' plays an important role in the interface between the aqueous solution and the aggregate's core (*39–41*). AMTPS appear when the surfactants present in aqueous solution are able to form two macroscopic phases under specific conditions. These systems are dependent on temperature and surfactant concentration, displaying a single phase below a temperature (*40*), known as cloud point temperature (*42*) or T_{cloud} (*41*). As graphically represented in **Figure 1.a)**, above T_{cloud}, the phase separation occurs, and thus AMTPS are composed of two distinct phases, one micelle-rich and one micelle-poor phase, that can be either the top or bottom layers, depending on the surfactant adopted (*39–42*). The phase separation behavior for different surfactants can be described by establishing the

binodal curves, *i.e.* plotting T_{cloud} *versus* surfactant concentration, which represent the boundary between the conditions at which the system presents a single phase (below/outside the curve) or two macroscopic phases (above/inside the curve) (see **Figure 1.b)**) (*40*). It should be pointed out that the surfactants employed can be either ionic (cationic (*43*) and anionic (*43*)) or non-ionic (*44*). Meanwhile, some additives, depending on their physico-chemical properties were shown to affect the phase separation behavior of surfactant-based mixtures (*45*, *46*).

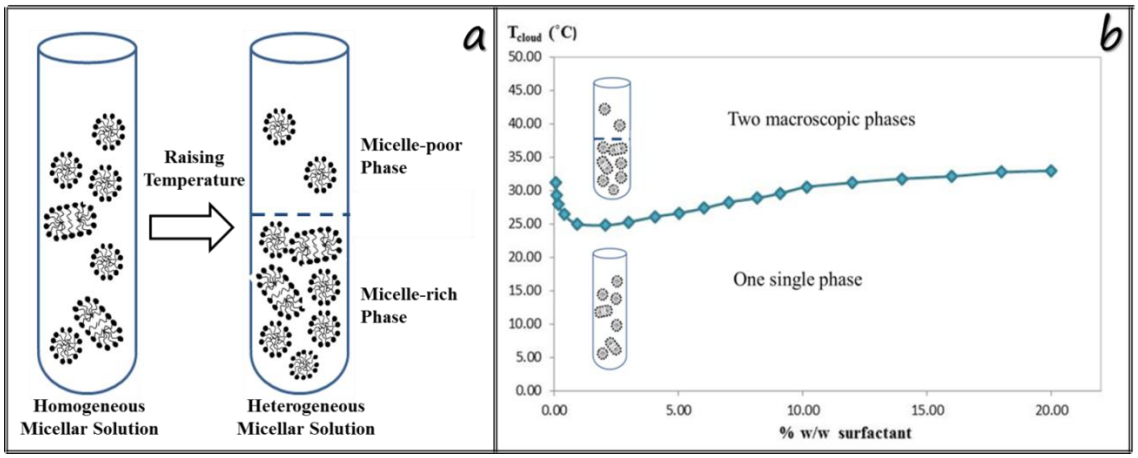

Figure 1.a) Schematic illustration of a particular AMTPS composed by Triton X-114, in which a temperature raise leads to two phase generation; **b)** Binodal curve of Triton X-114 + McIlvaine buffer pH 7. Above/inside the binodal curve the system displays two macroscopic phases, while below/outside the binodal curve only a single phase is depicted.

The pioneering work of Bordier (*47*), in which the differential partitioning of a plethora of proteins within AMTPS phases was successfully carried out, triggered the publication of many other works applying this type of systems in bioseparation. Since then, not only the separation, concentration and purification of several proteins using AMTPS were addressed (*39–41*, *48*, *49*), but also of a wider array of biocompounds such as viruses (*39*), DNA (*50*), bacteriocins (*51*), antibiotics (*52*) and porphyrins (*53*). Moreover, Kamei and co-workers (*54*) focused on the balance of interactions affecting the effectiveness of such systems and proved that the electrostatic forces between biomolecules and micelles play a crucial role in the migration phenomenon in AMTPS composed of a pair of distinct surfactants. The authors brought new evidences that this technique could be an enhanced route for the selective extraction, if properly designed. Based on this concept, this work envisages the exploitation of AMTPS by introducing

ILs as the second surfactant (co-surfactant) and their use and application as extraction technologies and analytical techniques.

The application of ILs in AMTPS playing the co-surfactant role can be supported by the evidences introduced by Bowers *et al.* (*55*). The authors described the possibility of ILs to self-aggregate due to the presence of long (enough) alkyl side chains, turning them into amphiphilic molecules. Since then, a number of authors have studied the aggregation and micelle formation of ILs in aqueous solutions (*56–60*), their incorporation in mixed micelles (*58–66*) and their contribution to the modification of the physicochemical properties of surfactant micelles (*56*, *58–66*). ILs with long alkyl chains were also found to be able to self-aggregate, promoting significant increments in the enzymatic activity (*67*). The addition of ILs to a surfactant can either decrease (*58*, *61*, *63*) or increase (*60*, *64*, *65*) the CMC and also affect the aggregation number (*55*, *56*, *61*), depending on the ILs structural features (alkyl side chain, cation and anion) and the surfactant head group (*58*, *61*, *66*). The ILs ability to act as surfactants has been evaluated by the determination of their CMCs by applying several methods, such as, electric conductivity (*55–57*, *59*, *61*, *63*), surface tension (*55*, *60*, *64*, *66*), fluorescence (*56*, *58*) and isothermal titration calorimetry (*57*, *63*) measurements.

Considering the big picture of AMTPS application, their design should be carefully conducted. It should be firstly considered the chemical, physical and biological properties of the target molecules; the main surfactant (anionic, nonionic or cationic) and the IL as co-surfactant must be tuned to instil an appropriate environment and to develop the binodal curves. The addition of buffered solutions also plays a major role in the system since it controls the presence of charged/uncharged species of the molecules extracted in aqueous solution. Thus, different combinations of phase forming agents lead to different effects on the T_{cloud}, comparing to the traditional AMTPS employing just the surfactant. For that purpose this technology must be successful in the extraction of both hydrophilic and hydrophobic solutes. It should be stressed that not only the extractive capability of the AMTPS, but also the effect of the components and operational conditions on the stability of the target molecules should be assessed. A schematic illustration of a possible strategy designed to develop efficient AMTPS-based platforms is presented in **Figure 2**.

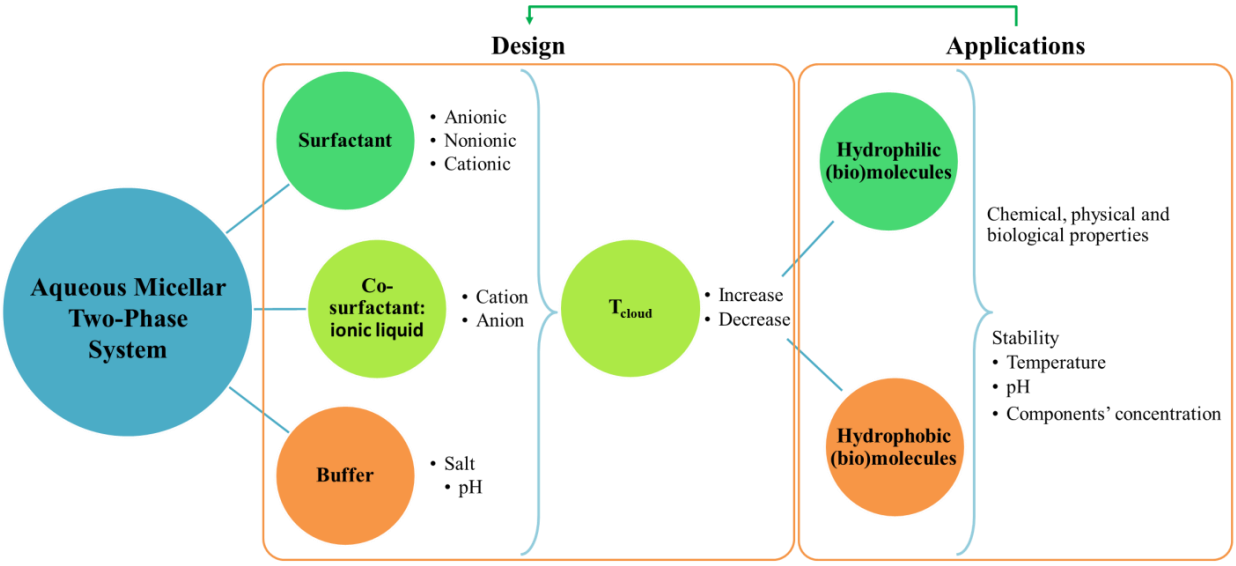

Figure 2. Schematic representation of a strategy for the appropriate design and application of AMTPS.

1.2. SCOPE AND OBJECTIVES

Pioneering studies have already demonstrated the potential of ILs to act as surfactants. However, there is no experimental evidence of their use in the formation of AMTPS and their application as liquid-liquid extraction methodologies. In this sense, this work intends to propose a new contribution in this domain, presenting the design of a new class of AMTPS which use ILs as co-surfactants and the evaluation of their potential as extractive platforms for distinct (bio)molecules. It addresses the development of new systems based in a common surfactant and ionic liquids as co-surfactants, helping in the formation of the two aqueous phases and their extractive and analytical performances in the separation and analysis of different molecules.

This thesis will be organized according to distinct chapters in article format. A general introduction is presented in CHAPTER 1, which presents the state-of-the-art considering different systems already used and studied in terms of liquid-liquid extraction technologies, including ATPS specifically, AMTPS and their main applications.

In CHAPTER 2, the binodal curves of Triton X-114 + McIlvaine buffer at pH 7 + 10 different ILs belonging to three distinct families, imidazolium, phosphonium and quaternary ammonium, were established to be employed as (bio)separation processes. The solubility curves of such systems were designed to evaluate the impact of the presence of each of the pre-selected ILs as a co-surfactant in conventional surfactant/salt-based AMTPS. However, not only the family of IL was tested, but also the ILs' concentration (0.3 and 0.5 wt%) and some of their structural features (cation, anion and alkyl chain). As proof of concept, these new AMTPS developed with ILs were evaluated in the selective separation of Cytochrome c (Cyt c) and Rhodamine 6G (R6G), studied as model compounds with different levels of chemical complexity and distinct finalities.

CHAPTER 3 shows a different application for some of the AMTPS designed, specifically those applying imidazolium- and phosphonium-based ILs. These liquid-liquid extraction systems were applied in the separation of a natural colorant called curcumin from its vegetal extract, a more complex matrix. The main objective in this work was the study of the impact of the ILs' cation and the IL concentration on the extraction parameters, recovery and partition coefficient. First of all, the stability of the natural colorant was investigated considering the different ILs and operational conditions studied in the extraction step, to access the chemical structure and activity of the

molecule during the extraction studies. In this part of the work, the effects of different IL concentrations, the presence of Triton X-114 and different times of exposure of the colorant were investigated.

CHAPTER 4 describes the use of AMTPS in the context of analytical chemistry as a more sustainable pre-treatment route for the re-concentration of molecules in aqueous solution. In this specific work, the AMPTS were used as platform for the re-concentration of tenofovir disoproxil fumate (TDF), an antiretroviral used in HIV/AIDS treatment. In what regards the application of AMTPS, the presence/absence of ILs as a co-surfactant, the IL family (imidazolium and phosphonium) and the minimization of the Triton X-114 concentration were the conditions tested. A parallel strategy was proposed by applying common aqueous two-phase systems based in polymer + salt + water systems. In this sense, the polymer polyethylene glycol with a molecular weight of 600 $g.mol^{-1}$ (PEG 600) and two distinct salts, either the sodium sulphate, Na_2SO_4 (inorganic) or the ammonium citrate, $(NH_4)_3C_6H_5O_7$ (organic) were tested. Besides the impact of the "salting-out" salt agent nature on the extraction ability, also the concentration of the polymer and the salt were taken into account to evaluate the better system to be applied in the extraction of the antiretroviral from the real matrix, the human plasma.

For a better understanding, and aiming at the complete clarification of this issue, it should be stressed that all experiments as well as the preparation of the article corresponding to the CHAPTER 2 were entirely performed by Filipa Vicente. In CHAPTER 3 and CHAPTER 4, the work was done in a close collaboration with Profa. Dra. Valéria de Carvalho Santos Ebinuma from Faculdade de Ciências Farmacêuticas, Universidade Estadual Paulista, UNESP (Brazil) and with Prof. Dr. José Alexsandro da Silva from Departamento de Farmácia, Universidade Estadual da Paraíba, UEPB (Brazil), respectively. Some of the AMTPS developed during CHAPTER 2 were used according with the specific goals of each project and collaborator. The contribution of the candidate in both projects involved the stability tests and the partitioning studies of curcumin by applying the AMTPS and the extraction experiments of the antiretroviral using the AMTPS, as well as the preparation of the two articles.

2. DESIGN OF NOVEL AQUEOUS MICELLAR TWO-PHASE SYSTEMS USING IONIC LIQUIDS AS CO-SURFACTANTS FOR THE SELECTIVE EXTRACTION OF (BIO)MOLECULES

Separation and Purification Technology, 2014, accepted

2.1. INTRODUCTION

The first step of every extraction process involving AMTPS is the determination of the binodal curves. The information gathered allows the choice of one or more (two-phase) mixture compositions and the evaluation of several parameters related with the partition phenomenon, *e.g.* partition coefficient, extraction efficiency and recovery of the specific target molecules.

Cyt c is a heme protein present in the inner membrane of mitochondria and it is vital to the normal cell functioning, since it is involved in both life and death processes of the cells. Among several functions, its involvement in the oxidative phosphorylation by the electron transport chain to generate energy and its contribution in the apoptose are by far the more important (well-reviewed in (*68*)). R6G is an organic (*69*) and cationic (*70*) dye with additional fluorescence properties (*69*, *70*). This feature makes it extensively applied in several areas of expertise, from the textile industry (*71*) to the fluorescence microscopy and spectroscopy (*69*, *70*).

In this section, a novel class of AMTPS based on the nonionic surfactant Triton X-114 as the main surfactant, the McIlvaine buffer and several ILs acting as co-surfactants, is proposed. Moreover the potential of these AMTPS was evaluated to be used in (bio)separation process, by investigating their capacity to selectively separate Cyt c R6G, used here as model compounds.

2.2. EXPERIMENTAL SECTION

2.2.1. Materials

The imidazolium-based ILs 1-decyl-3-methylimidazolium chloride [C_{10}mim]Cl (purity > 98 wt%), 1-dodecyl-3-methylimidazolium chloride [C_{12}mim]Cl (purity > 98 wt%) and 1-methyl-3-tetradecylimidazolium chloride [C_{14}mim]Cl (purity > 98 wt%) were acquired at Iolitec (Ionic Liquid Technologies, Heilbronn, Germany). All the phosphonium-based ILs, namely trihexyltetradecylphosphonium chloride [$P_{6,6,6,14}$]Cl (purity = 99.0 wt%), trihexyltetradecylphosphonium bromide [$P_{6,6,6,14}$]Br (purity = 99.0 wt%), trihexyltetradecylphosphonium decanoate [$P_{6,6,6,14}$][Dec] (purity = 99 wt%), trihexyltetradecylphosphonium dicyanamide [$P_{6,6,6,14}$][$N(CN)_2$] (purity = 99.0 wt%), trihexyltetradecylphosphonium bis (2,4,4-trimethylpentyl)phosphinate [$P_{6,6,6,14}$][TMPP] (purity = 93.0 wt%) and tetraoctylphosphonium bromide [$P_{8,8,8,8}$]Br (purity = 95.0 wt%) were kindly supplied by Cytec. The ammonium-based IL tetraoctylammonium bromide [$N_{8,8,8,8}$]Br (purity = 98 wt%) was purchased from Sigma-Aldrich®. The chemical

structures of the cations and anions composing the list of ILs herein investigated are depicted in **Figure 3a**, Triton X-114 (laboratory grade) was supplied by Sigma-Aldrich® and the McIlvaine buffer components, namely sodium phosphate dibasic anhydrous Na_2HPO_4 (purity ≥ 99%) and citric acid anhydrous $C_6H_8O_7$ (purity = 99.5%) were acquired at Fisher Chemical and Synth, respectively. The Cyt c from horse heart (purity ≥ 95 wt%) and R6G (purity ≈ 95 wt%),depicted in **Figure 3b** were both acquired at Sigma-Aldrich®.

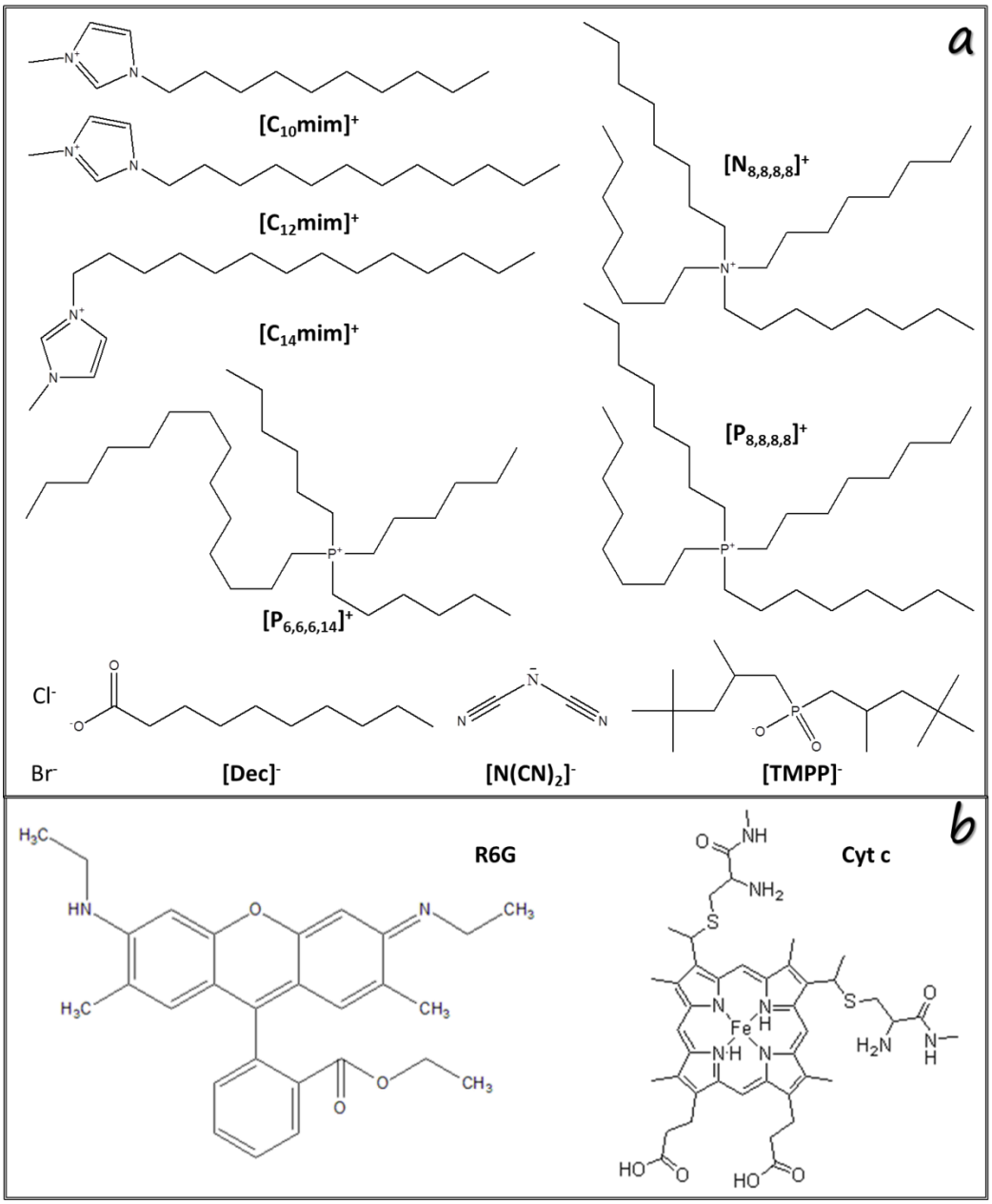

Figure 3. Chemical structure representation of **a)** cations and anions composing the ILs and **b)** R6G and Cyt c used in this work, plus the respective abbreviations.

2.2.2. Methods

2.2.2.1. Binodal curves

The binodal curves of the AMTPS composed of Triton X-114 and the McIlvaine buffer at pH 7 (82.35 mL of 0.2M Na_2HPO_4 + 17.65 mL of 0.1M $C_6H_8O_7$), using different ILs as co-surfactants were determined using the cloud point method, whose experimental protocol is well described in literature (*72*). This methodology consists of a visual identification, while raising the temperature of the point at which a mixture with known composition becomes turbid and cloudy, *i.e.* T_{cloud}. Then, the experimental binodal curves were obtained by plotting the T_{cloud} *versus* the surfactant concentration (mass units). The knowledge acquired from them allows the selection of strategic mixture points which correspond to the biphasic region. This biphasic region represents the zone of temperature *versus* surfactant mass concentration where the micelles are formed. All binodal curves were determined at least in triplicate, and the respective standard deviations calculated.

2.2.2.2. Partitioning studies of Cyt c and R6G by applying AMTPS

The AMTPS used in the partitioning studies of both Cyt c and R6G were gravimetrically prepared in glass tubes by weighing specific amounts of each component: 10 wt% of Triton X-114 + 0 wt%, 0.3 wt% or 0.5 wt% of each IL tested, being the McIlvaine buffer solution at pH 7 used to complete a final volume of 10 mL. To each system, the appropriate amount of each one of the model (bio)molecules was added: 10 wt% of an aqueous solution of Cyt c (*at circa* 2.0 $g.L^{-1}$) and approximately 0.30 mg of the R6G dye powder. The systems were homogenized at least for 2 hours in the freezer at 7 ºC, using a tube rotator apparatus model 270 from Fanem®, avoiding the turbidity of the system. Then, the systems were left at 35 ºC overnight, allowing the thermodynamic equilibrium to be reached, thus completing the separation of the phases as well as the migration of the model molecules. At the conditions adopted in the present work, the systems resulted in a micelle-rich and a micelle-poor as the bottom and top layers, respectively. Both phases were carefully separated and collected for the measurement of volume, viscosity, and quantification of the model molecules. The UV spectroscopy was elected to quantify each molecule at 409 nm for Cyt c and 527 nm for R6G, using a Molecular Devices Spectramax 384 Plus | UV-Vis Microplate Reader. The analytical quantifications were performed in triplicate and at least three parallel assays

for each system were done, being the average values and the respective standard deviations presented. Possible interferences of the AMTPS components (Triton X-114, McIlvaine buffer or IL when present) within the analytical quantification method were investigated and prevented through routinely applying blank controls. Thus, the partition coefficients for Cyt c ($K_{Cyt\ c}$) and R6G (K_{R6G}) were calculated as the ratio between the amount of each compound present in the micelle-rich (bottom) and the micelle-poor (top) phases, as described in Eqs. 1 and 2.

$$K_{Cyt\ c} = \frac{[Cyt\ c]_{Bot}}{[Cyt\ c]_{Top}} \quad \text{(Eq. 1)}$$

where $[Cyt\ c]_{bot}$ and $[Cyt\ c]_{bot}$ are, respectively, the concentration of Cyt c (in $g.L^{-1}$) in the bottom and top phases.

$$K_{R6G} = \frac{Abs_{Bot}^{R6G}}{Abs_{Top}^{R6G}} \quad \text{(Eq. 2)}$$

where Abs_{Bot}^{R6G} and Abs_{Top}^{R6G} are the absorbance data of R6G in the bottom and top phases, respectively. It should be stressed that the concentration of Cyt c in each phase was determined based on a calibration curve previously established. However, due to practical limitations that disallowed the determination of a calibration curve for R6G, the K_{R6G} was calculated taking into consideration the final values of Abs in both phases. The recovery (R) parameters of each molecule towards the bottom (R_{Bot}) and the top (R_{Top}) phases were determined following Eqs. 3 and 4:

$$R_{Bot} = \frac{100}{1+\left(\frac{1}{R_v \times K}\right)} \quad \text{(Eq.3)}$$

$$R_{Top} = \frac{100}{1+R_v \times K} \quad \text{(Eq.4)}$$

where R_v stands for the ratio between the volumes of the bottom and top phases. Finally, the selectivity ($S_{R6G/Cyt\ c}$) of the AMTPS herein developed was described as the ratio between the K values found for R6G and Cyt c, as indicated in Eq. 5:

$$S_{R6G/Cyt\ c} = \frac{K_{R6G}}{K_{Cyt\ c}} \quad \text{(Eq. 5)}$$

2.2.2.3. Viscosity measurements of both phases

The viscosity was measured using an automated SVM 3000 Anton Paar rotational Stabinger viscosimeter-densimeter at 25 ºC and at atmospheric pressure for each top and bottom phases of the entire set of AMTPS studied.

2.3. RESULTS AND DISCUSSION

2.3.1. Binodal curves with ILs acting as co-surfactants

The first step of this work consisted on the determination of the binodal curves of AMTPS with several ILs as co-surfactants (*73*), which knowledge is essential not only to perform the partitioning studies, but also to optimize the operational conditions of the separation process. Therefore, the binodal curves were established through visual identification of the T_{cloud} for all the mixtures composed of Triton X-114, McIlvaine buffer, either in the absence or presence of IL. During the binodal curves determination, the effect of the presence of different ILs as co-surfactants was assessed, and with it, several ILs chemical features were strategically considered, namely the alkyl side chain length, the anion structure and the cation conformation, and the ILs' mass concentration, being their impact minutely discussed in the next sections.

2.3.1.1. Effect of the ILs' on the AMTPS bimodal curves

A set of ten distinct ILs, belonging to the imidazolium ($[C_n mim]^+$ with n = 10, 12 and 14), phosphonium ($[P_{6,6,6,14}]^+$ and $[P_{8,8,8,8}]^+$) and ammonium ($[N_{8,8,8,8}]^+$) families, were applied as co-surfactants in AMTPS based in Triton X-114 and the McIlvaine buffer. The experimental binodal curves obtained are depicted in **Figures 4 and 5**, revealing that the presence of different ILs affects the phase separation either increasing or decreasing the T_{cloud}. In this sense, ILs can be divided into two main groups related with the impact on phase formation, when compared to the original AMTPS (Triton X-114 + McIlvaine buffer). The first group involves the imidazolium-based ILs, more hydrophilic, which produce an increase in the T_{cloud}. The second group, which covers the phosphonium- and quaternary ammonium-based ILs, more hydrophobic, that induce significant reductions in the T_{cloud} (*74*). The opposite trends here verified are attributed to the main interactions competing and governing the phase separation phenomenon in these specific AMTPS. In fact, this phenomenon is complex and is strongly dependent

of the balance involving the hydration degree of the surfactant chain and the electrostatic interactions among the charged head group (*75*). Concerning the first group, it can be related with the greater hydration shell present around the imidazolium-based ILs and consequent higher energy required to separate the system into two macroscopic phases (*65*) or with the IL head group that may charge the micellar surface, thus generating electrostatic repulsion between them (*76*). In this manner, ILs with stronger hydrophobic nature lead to smaller micellar hydration shells enhancing the ability to undergo phase separation at lower temperatures (*44*). The picture emerging from these data indicates that the most hydrophobic ILs, independently of their concentration, seem to be more advantageous co-surfactants from an operational point of view, since lower temperatures are better for (bio)separation processes.

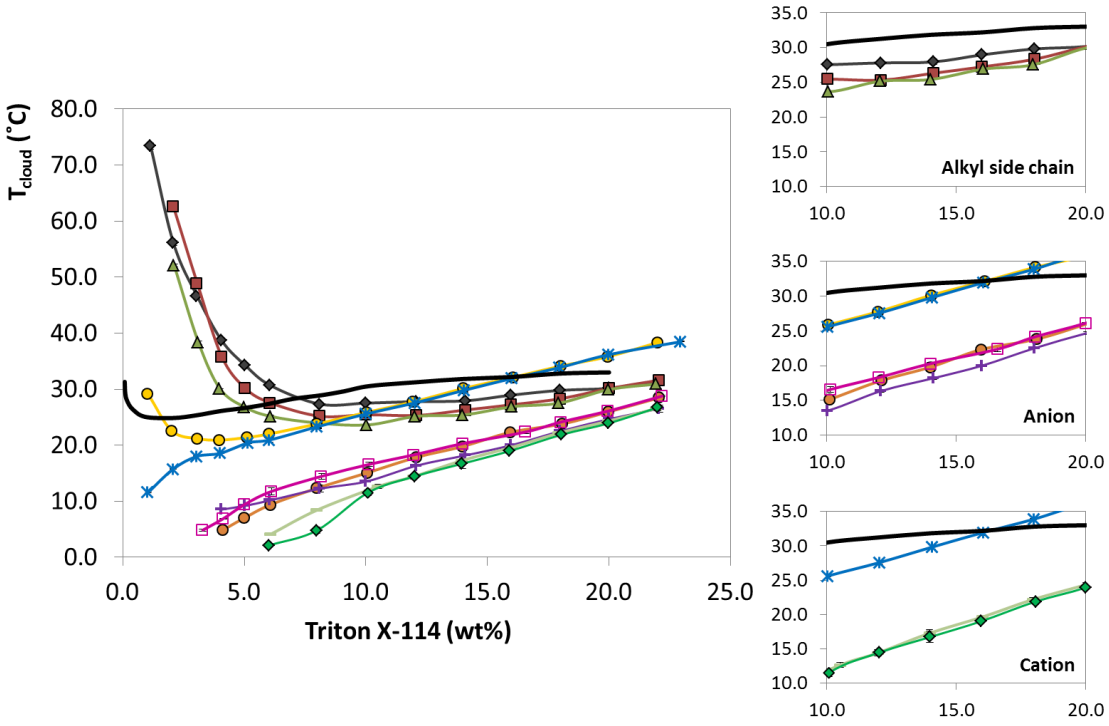

Figure 4. Binodal curves for the studied ILs at 0.3 wt%, at pH 7: —, without IL; ◆, [C_{10}mim]Cl; ■, [C_{12}mim]Cl; ▲, [C_{14}mim]Cl; ●, [$P_{6,6,6,14}$]Cl; ✳, [$P_{6,6,6,14}$]Br; ●, [$P_{6,6,6,14}$][Dec]; ┼, [$P_{6,6,6,14}$][$N(CN)_2$]; □, [$P_{6,6,6,14}$][TMPP]; —, [$P_{8,8,8,8}$]Br; ◆, [$N_{8,8,8,8}$]Br. The effect of ILs' structural features is provided separately in the insets to facilitate the analysis.

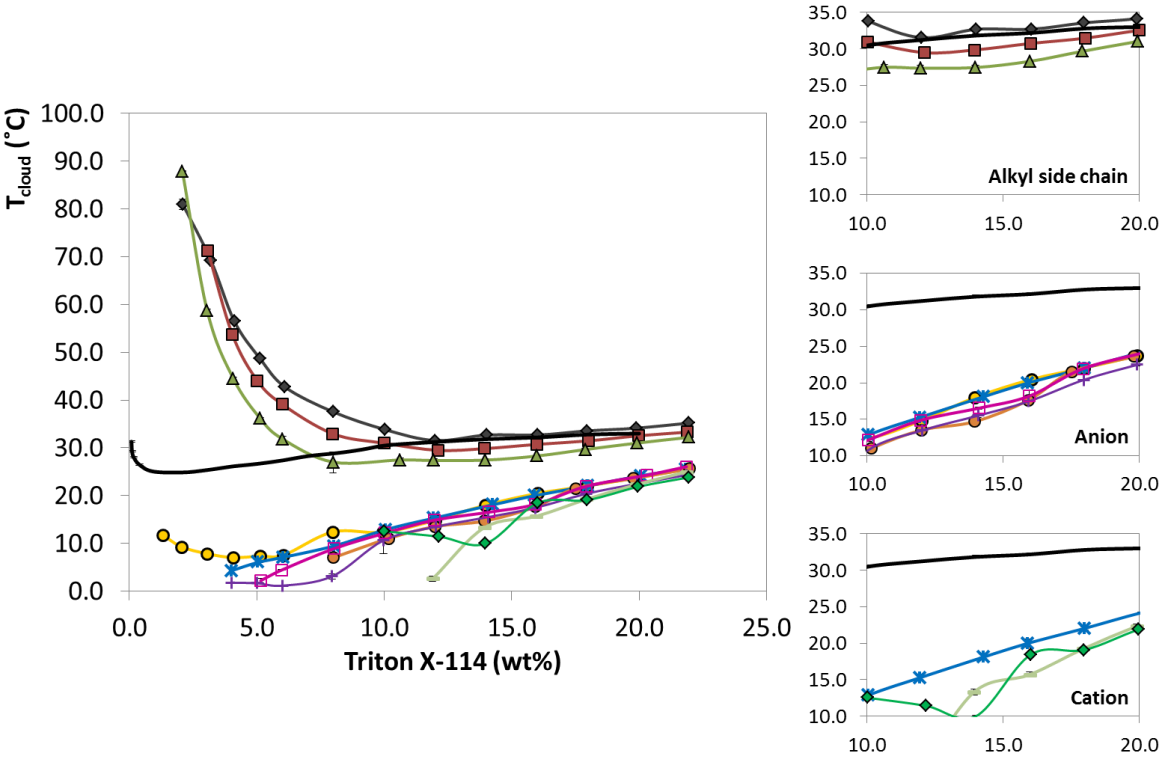

Figure 5. Binodal curves for the studied ILs at 0.5 wt%, at pH 7: —, without IL; ◆, [C_{10}mim]Cl; ■, [C_{12}mim]Cl; ▲, [C_{14}mim]Cl; ●, [$P_{6,6,6,14}$]Cl; ✳, [$P_{6,6,6,14}$]Br; ●, [$P_{6,6,6,14}$][Dec]; ┼, [$P_{6,6,6,14}$][$N(CN)_2$]; □, [$P_{6,6,6,14}$][TMPP]; —, [$P_{8,8,8,8}$]Br; ◆, [$N_{8,8,8,8}$]Br. The effect of ILs' structural features is provided separately in the insets to facilitate the analysis.

2.3.1.2. Effect of the ILs' structural features

Aiming at designing more efficient ILs to be applied as co-surfactants in Triton X-114 + McIlvaine buffer-based AMTPS several modifications at the level of the alkyl side chain, the anion moiety and the cation core were conducted. In order to address the impact of the alkyl side chain of the cation on the phase separation behavior, three [$C_n$mim]Cl-based ILs were selected, varying their *n* value from 10 to 14 carbon atoms. Their comparative representation is depicted in **Figures 4 and 5** and it is possible to observe that, independently of the mass concentration of IL added, 0.3 wt% or 0.5 wt%, the capability to generate two phases increases according to the trend [C_{10}mim]Cl < [C_{12}mim]Cl < [C_{14}mim]Cl – *i.e.* resulting from the increasing hydrophobicity of the IL. This increasing ability to create AMTPS is a result from the lower number of water molecules around the micelles hampering their grouping in one phase, leading to less energy requirements to undergo phase separation and, consequently, lower T_{cloud} (*77*), which is in agreement with evidences found in literature, related with the easier

aggregation of the molecules with longer alkyl chain lengths (lower Gibbs energy) (*56*) and with the benign impact of the lipophilicity on the T_{cloud} (*57*). As expected, this effect is even stronger for $[P_{6,6,6,14}]Cl$, due to its enhanced hydrophobicity.

The influence of the anion moiety on the coexistence curves was addressed by using five different ILs sharing the $[P_{6,6,6,14}]^+$ cation, namely $[P_{6,6,6,14}]Cl$, $[P_{6,6,6,14}]Br$, $[P_{6,6,6,14}][Dec]$, $[P_{6,6,6,14}][N(CN)_2]$ and $[P_{6,6,6,14}][TMPP]$. This group of ILs induces a decrease in T_{cloud} of the Triton X-114 + McIlvaine buffer-based AMTPS, as aforementioned; however, the intensity of this behaviour depends on the anion nature. The graphical representation of such binodal curves is reported in **Figures 4 and 5** in the insets. Apart from the fact that at higher IL mass concentrations, the anion influence is scattered (**Figure 5**), at 0.3 wt% of IL is possible to notice that the ability to form two phases increases in the order $[P_{6,6,6,14}]Cl \approx [P_{6,6,6,14}]Br << [P_{6,6,6,14}][TMPP] \approx [P_{6,6,6,14}][Dec] < [P_{6,6,6,14}][N(CN)_2]$. This tendency shows the existence of a clear distinction between the more hydrophilic (Cl^- and Br^-) and the more hydrophobic anions ($[TMPP]^-$, $[Dec]^-$ and $[N(CN)_2]^-$). It should be stressed that, for Cl^- and Br^- at low concentrations of Triton X-114, a more prominently distinct behavior was observed being the Br^- anion responsible for major T_{cloud} decreases. This behavior could be related to the higher ability of the Br^- to reduce the surface tension (*78*) or to the facilitate the Br^- adsorption into the micelles surface, reducing the electrostatic repulsion (*63*) and thus enhancing the molecules' tendency to self-aggregate, consequently forcing the reduction of the T_{cloud} values. When concerning the behavior induced by the remaining three anions, $[Dec]^-$, $[N(CN)_2]^-$ and $[TMPP]^-$, we attribute it to the fact that both anion and cation structures composing the IL would remain as part of the micellar structure, resulting in low micellar charge and thus, low electrostatic repulsion between them (*75*).

Finally, some modifications at the level of the cation, beyond the more hydrophilic *vs.* the more hydrophobic nature aforementioned, were considered. Those were connected with the change of the cation symmetry (from $[P_{8,8,8,8}]^+$ to $[P_{6,6,6,14}]^+$) or variation of the central atom from a phosphorous ($[P_{8,8,8,8}]^+$) to a nitrogen ($[N_{8,8,8,8}]^+$). As presented in **Figure 4** (inset), it is notorious that the symmetry is favorable to induce the ability to form AMTPS. Here again, the presence of higher concentrations of IL (**Figure 5** in the inset) deceases the effect of the structural modifications. When $[P_{8,8,8,8}]^+$ is compared with the $[N_{8,8,8,8}]^+$ cation, both possessing a strong hydrophobic nature, no significant

differences between their T_{cloud} behavior are noticed independently of the IL mass concentration studied (**Figures 4 and 5** in the insets).

2.3.1.3. Effect of the IL concentration

The impact of the concentration of ILs on the T_{cloud} behavior of Triton X-114 + McIlvaine buffer AMTPS was assessed by slightly increasing it from 0.3 wt% up to 0.5 wt%. In **Figure 6**, it is provided a comparison between the concentrations adopted in this study, being possible to observe, again, two distinct trends. One involving the imidazolium family (more hydrophilic nature) and other the phosphonium and quaternary ammonium chemical structures (more hydrophobic nature): higher concentration of ILs is converted either in an increase of the T_{cloud}, in the case of the imidazolium-based ILs, or in a reduction of the T_{cloud} for the phosphonium- and quaternary ammonium-based ILs. It should be pointed out that this change in T_{cloud} is relevant from both operational and economic points of view since very low amounts of ILs (used as co-surfactant) can significantly modify the T_{cloud} of the AMTPS. Even low amounts of [$C_n$mim]Cl-based ILs may be used to enhance the AMTPS performance, making them promising alternative approaches despite the higher T_{cloud} observed, for thermal stable molecules since the biphasic region is increased when compared to the AMTPS without IL, thus offering more appealing extraction conditions.

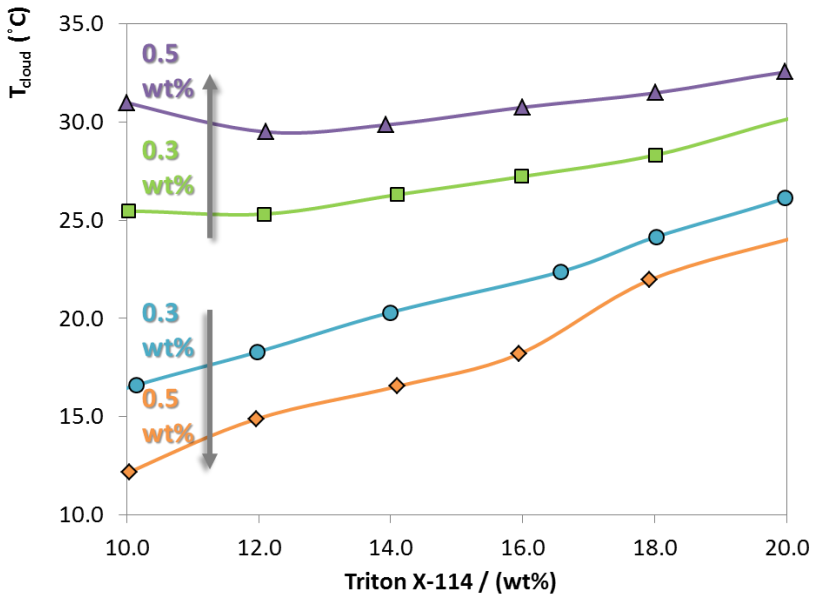

Figure 6. Influence of the IL' mass concentration on the T_{cloud} of AMTPS using more hydrophilic (imidazolium-based) or more hydrophobic (phosphonium-based) ILs: ■, [C_{12}mim]Cl at 0.3 wt%; ▲, [C_{12}mim]Cl at 0.5 wt%; ●, [$P_{6,6,6,14}$][TMPP] at 0.3 wt%; ◆, [$P_{6,6,6,14}$][TMPP] at 0.5 wt%. [C_{12}mim]Cl and [$P_{6,6,6,14}$][TMPP] were selected as examples to indicate the common trend for both distinct groups of ILs.

2.3.2. Application of the designed AMTPS to the selective extraction of Cyt c and R6G

The separation of Cyt c and R6G was attempted by applying these novel AMTPS using ILs as co-surfactants. The partitioning studies of these molecules were performed using AMTPS composed of 10 wt% of Triton X-114 in the absence and presence of 0.3 wt% and 0.5 wt% of ILs. Being important from a technological point of view, a characterization of the viscosity of the resulting phases is reported in **Table 1**. The results indicate that the presence of the ILs contributes to slightly reduce the viscosity of the bottom phase (micelle-rich phase) in most of the AMTPS.

The results regarding the partition behavior of the targeted molecules are reported in **Table 2**. It should be mentioned that in some cases, experimental limitations precluded the execution of the partitioning studies hindering the determination of partition coefficients and other parameters. It is clearly observed in the results obtained the preferential migration of Cyt c to the micelle-poor phase ($\log K_{Cyt\ c} < 0$), while the R6G is migrating to the micelle-rich phase ($\log K_{R6G} > 0$). These opposite migration tendencies can be easily understood based on a balance involving hydrophobic, electrostatic and excluded-volume interactions between the targeted molecules and the micelles. As the Cyt c is a hydrophilic protein, it presents a higher affinity for the more hydrophilic layer (micelle-poor phase), which is in agreement with literature (*47*). Also, its isoelectric point – 10.65 (*79*) – is higher than the pH herein adopted (McIlvaine buffer at pH 7), meaning that the protein is positively charged under this set of process conditions. In this sense, electrostatic interactions seem to play an important role in the partition of Cyt c, since the IL, especially its cation, may force the protein migration towards the micelle-poor layer. Moreover, excluded-volume interactions may also interfere in the partition tendency of Cyt c, especially for higher micelle concentrations that lead to lower volume available in the micelle-rich layer, forcing its migration towards the micelle-poor phase. Meanwhile, R6G is migrating preferentially for the micelle-rich phase, since this small molecule (*80*) is a neutral species at pH 7; in this case hydrophobic interactions are controlling the molecule partitioning behavior. A more detailed discussion can be performed by carefully analyzing the impact of different conditions (IL's nature and concentration) on the partitioning of Cyt c. When taking a closer look at the [$C_n$mim]Cl-based ILs as co-surfactants, it is possible to conclude that the migration increases with the elongation of the alkyl chain length (at

Table 1. Viscosity measurements for all the studied AMTPS in presence and absence of each one of the ILs studied, at 25 ± 1°C.

System	wt% IL	Phase	Viscosity (mPa.s)
Without IL – Triton X-114 only	---	Top	1.04
		Bottom	244.13
[C_{10}mim]Cl	0.3	Top	1.05
		Bottom	180.39
	0.5	Top	1.23
		Bottom	92.19
[C_{12}mim]Cl	0.3	Top	1.05
		Bottom	207.04
	0.5	Top	1.06
		Bottom	167.52
[C_{14}mim]Cl	0.3	Top	1.04
		Bottom	224.76
	0.5	Top	1.05
		Bottom	197.62
[$P_{6,6,6,14}$]Cl	0.3	Top	1.05
		Bottom	229.68
	0.5	Top	1.03
		Bottom	225.74
[$P_{6,6,6,14}$]Br	0.3	Top	1.07
		Bottom	226.85
	0.5	Top	1.04
		Bottom	217.02
[$P_{6,6,6,14}$]Dec	0.3	Top	1.06
		Bottom	210.27
	0.5	Top	1.05
		Bottom	188.74
[$P_{6,6,6,14}$]$N(CN)_2$	0.3	Top	1.03
		Bottom	209.41
[$P_{6,6,6,14}$]TMPP	0.3	Top	1.05
		Bottom	210.91
	0.5	Top	1.06
		Bottom	190.19
[$P_{8,8,8,8}$]Br	0.3	Top	1.04
		Bottom	196.96
	0.5	Top	1.08
		Bottom	171.19
[$N_{8,8,8,8}$]Br	0.3	Top	1.06
		Bottom	215.68

0.3 wt% of IL is -0.52 ± 0.02 < log $K_{Cytc\ c}$ < -0.69 ± 0.02 and at 0.5 wt% is -0.24 ± 0.04 < log $K_{Cytc\ c}$ < -0.52 ± 0.05), as shown in previous studies (*81*). This behavior can be justified by the intensification of the excluded-volume interactions as the ILs' hydrophobicity increases (*8, 27*). When the concentration of the entire series of [$C_n$mim]Cl-based ILs increases to 0.5 wt%, the $K_{Cyt\ c}$ decreases (for example for [C_{10}mim]Cl, log $K_{Cyt\ c}$ varies from -0.52 ± 0.02 to -0.24 ± 0.04), probably as a result of operational limitations related with the proximity between the separation temperature (35 ˚C) and the T_{cloud} (33.82 ± 0.06 ºC). Finally, in presence of the phosphonium-based ILs, especially 0.5 wt% of [$P_{8,8,8,8}$]Br, the protein is even more extracted to the micelle-poor phase (log $K_{Cytc\ c}$ = -1.51 ± 0.14). Besides, and contrarily to the behavior observed with the [$C_n$mim]Cl-based ILs, increasing the concentration of IL, the $K_{Cyt\ c}$ is also increasing (*e.g.* for [$P_{8,8,8,8}$]Br the log $K_{Cyt\ c}$ varies from -1.08 ± 0.13 to -1.51 ± 0.14). Again, these facts are corroborating the strong dependence on the hydrophobic character of the ILs, which may increase the micelles concentration, employing a more pronounced excluded-volume effect on the protein. In addition, the recovery values (regarding the phase where each molecule is more concentrated), reported in **Figure 7** corroborate the opposite migration of Cyt c to the micelle-poor phase (18.04 ± 2.80 % < R_{Top} < 98.42 ± 0.54 %) and R6G to the micelle-rich phase (96.12 ± 0.15 % < R_{Bot} < 99.70 ± 0.19 %). It should be noted that the low R_{Top} values obtained in presence of the [$C_n$mim]Cl-based ILs are only related with the more deficient re-concentration of the Cyt c in one phase (K closer to the unit). As already described, it is notorious from the results of **Table 2** that, two distinct mechanisms explain the migration of the molecules here investigated, independently of the presence of ILs as co-surfactants. However, the results here presented also suggest that these partitions are improved by the addition of small amounts of the ILs studied. In fact, the partition of Cyt c in the conventional AMTPS (log $K_{Cyt\ c}$ = -0.59 ± 0.12), is less pronounced when compared to the novel ones (at 0.3 wt% of IL is -0.52 ± 0.02 < log $K_{Cytc\ c}$ < -1.08 ± 0.13 and at 0.5 wt% of IL is -0.24 ± 0.04 < log $K_{Cytc\ c}$ < -1.51 ± 0.14). Indeed, the use of ILs as co-surfactants truly enhances the extractive performance of these systems; still, when applying either [C_{10}mim]Cl or [$N_{8,8,8,8}$]Br at 0.3 wt% and the [$C_n$mim]Cl series at 0.5 wt% the partition can be decreased (-0.25 ± 0.04 < log $K_{Cyt\ c}$ < -0.56 ± 0.02).

Table 2. Logarithm function of $K_{Cyt\ c}$ and K_{R6G} by the application of all AMTPS studied, at weight fraction composition of 10 wt% of Triton X-114 and 0, 0.3 or 0.5 wt% of IL.

$$K_{R6G} = \frac{Abs^{R6G}{}_{Bot}}{Abs^{R6G}{}_{Top}} \qquad K_{Cyt\ c} = \frac{[Cyt\ c]_{Bot}}{[Cyt\ c]_{Top}}$$

	Bottom (Micelle-rich) Phase ← Log K_{R6G}		Log $K_{Cyt\ c}$ → Top (Micelle-poor) Phase	
	IL concentration			
	0.3 wt%	0.5 wt%	0.3 wt%	0.5 wt%
no IL	2.39 ± 0.30		-0.59 ± 0.12	
$[C_{10}mim]Cl$	2.14 ± 0.11	1.55 ± 0.06	-0.52 ± 0.02	-0.24 ± 0.04
$[C_{12}mim]Cl$	1.79 ± 0.10	1.99 ± 0.04	-0.68 ± 0.04	-0.43 ± 0.05
$[C_{14}mim]Cl$	2.65 ± 0.00	1.90 ± 0.14	-0.69 ± 0.02	-0.52 ± 0.05
$[P_{6,6,6,14}]Cl$	2.54 ± 0.02	2.16 ± 0.06	-0.82 ± 0.04	-0.90 ± 0.04
$[P_{6,6,6,14}]Br$	2.39 ± 0.05	2.07 ± 0.13	-0.85 ± 0.06	-1.02 ± 0.01
$[P_{6,6,6,14}][Dec]$	2.25 ± 0.24	2.47 ± 0.10	-0.84 ± 0.13	-1.02 ± 0.07
$[P_{6,6,6,14}][N(CN)_2]$	2.02 ± 0.10	---	-0.96± 0.28	---
$[P_{6,6,6,14}][TMPP]$	2.21 ± 0.21	2.13 ± 0.04	-1.03 ± 0.07	-0.90 ± 0.15
$[P_{8,8,8,8}]Br$	2.13 ± 0.04	---	-1.08 ± 0.13	-1.51 ± 0.14
$[N_{8,8,8,8}]Br$	1.70 ± 0.01	---	-0.56 ± 0.02	---

Finally, the preferential migration of the targeted molecules towards opposite phases of the AMTPS herein established can be reliably translated by means of their selectivity parameter ($S_{R6G/Cyt\ c}$). The results obtained are reported in **Figure 8** and suggest that the presence of ILs has a significant impact on the selectivity of this type of systems. In fact, when comparing the $S_{R6G/Cyt\ c}$ of the conventional AMTPS based in Triton X-114 plus McIlvaine buffer with the novel class possessing ILs acting as co-surfactant, an almost 4-fold enhancement, from 925.25 up to 3418.89, is achieved. Meanwhile, the results of **Figure 8** also suggest that the most advantageous $S_{R6G/Cyt\ c}$ conditions were obtained applying the AMTPS containing 0.3 wt% of either $[C_{14}mim]Cl$ ($S_{R6G/Cyt\ c}$ = 2224.06) or $[P_{6,6,6,14}]Cl$ ($S_{R6G/Cyt\ c}$ = 2295.81) and 0.5 wt% of $[P_{6,6,6,14}][Dec]$ ($S_{R6G/Cyt\ c}$ = 3418.89). The visual proof of their selectivity nature is depicted in **Figure 9**.

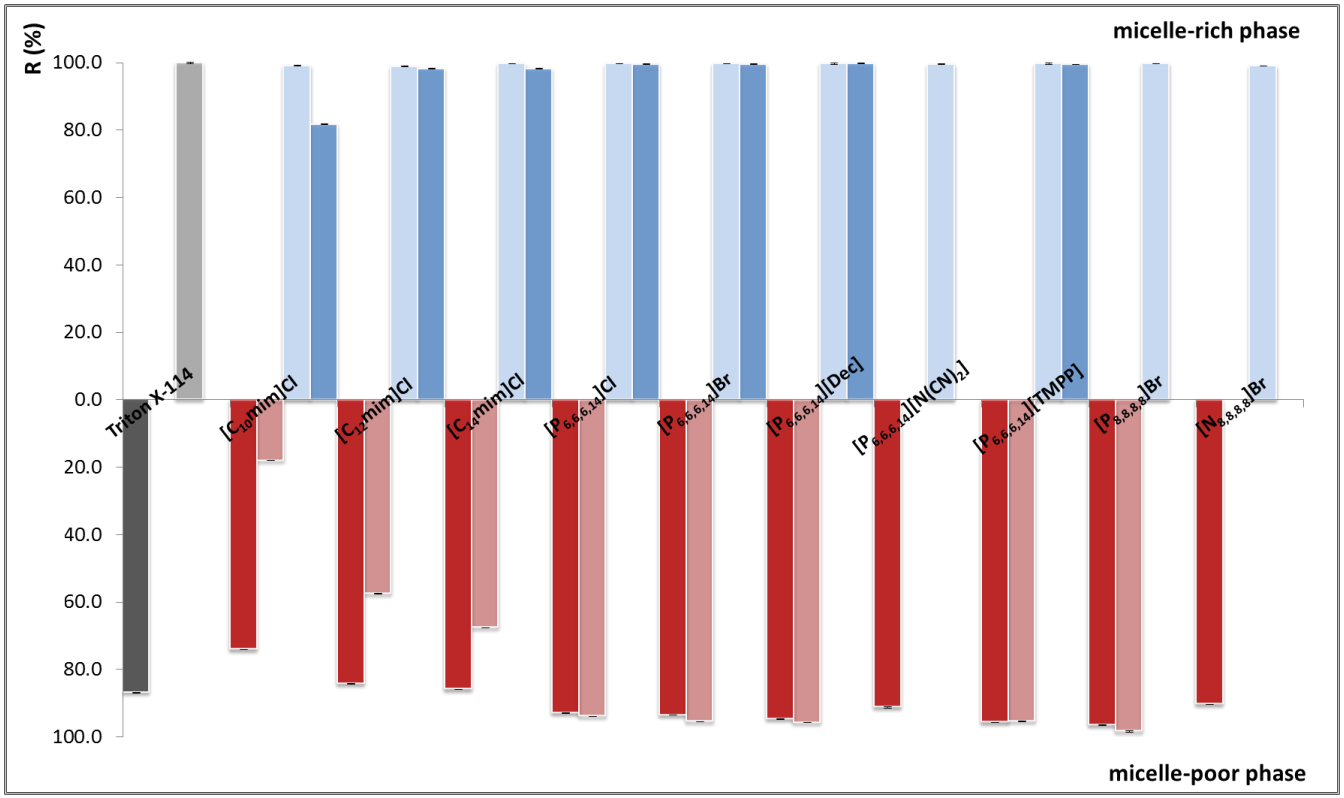

Figure 7. Recovery percentages for Cyt c and R6G by applying the AMTPS developed, at weight fraction composition of 10 wt% of Triton X-114 and 0.3 or 0.5 wt% of IL and: ■, log $K_{Cyt\ c}$ at 0.3 wt% IL; ■, log $K_{Cyt\ c}$ at 0.5 wt% of IL; ■, log K_{R6G} at 0.3 wt% IL; ■, log K_{R6G} at 0.5 wt% of IL.

Although the studies focusing on the partitioning of either R6G or Cyt c are limited, the performance of this novel process is here compared with other types of ATPS. The use of AMTPS with ILs as co-surfactants is capable of enhancing the extractive performance of R6G, independently of the concentration of IL employed ($1.55 \pm 0.06 < \log K_{R6G} < 2.65 \pm 0.00$ and $96.12 \pm 0.15\ \% < R_{Bot} < 99.70 \pm 0.19\ \%$), when compared to phosphonium-based ILs + tripotassium phosphate salt-based ATPS (log R6G values of -1.74, 0.56 and 0.90) (*82*). On the other hand, the extractive performance of Cyt c is also here boosted ($-0.24 \pm 0.04 < \log K_{Cytc} < -1.51 \pm 0.14$ and $18.04 \pm 2.80\ \% < R_{Top} < 98.42 \pm 0.54\ \%$), when compared with the results obtained by applying either imidazolium-based IL + potassium citrate buffer-based ATPS (extraction recoveries up to 94 %, by pH changes) (*81*) or the n-decyl tetra(ethylene oxide) + McIlvaine buffer-based AMTPS ($\log K_{Cyt\ c} \approx -0.09$) (*39*). These results show that AMTPS using IL as co-surfactants are promising techniques to be successfully applied in bioseparation processes and several fields of the pharmaceutical and biotechnological industries. Taking into account the industrial interest of these systems, a more profound investigation considering the recovery and recycling of the separation agents (surfactant and ILs) used is required, considering some of the techniques briefly described in literature (*83*, *84*).

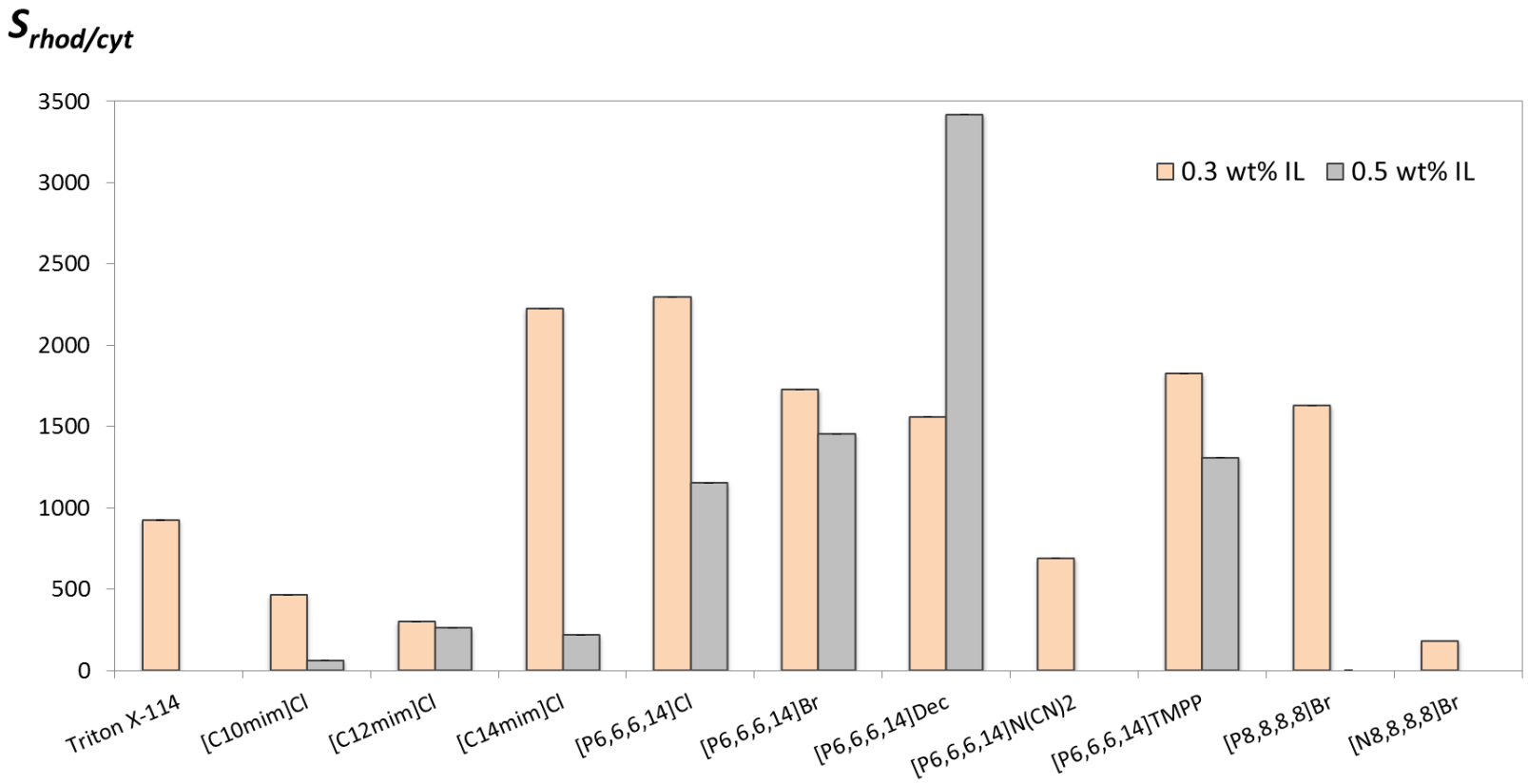

Figure 8. Selectivity results obtained through the application of all AMTPS studied for the extraction of R6G and Cyt c: ■, 0.3 wt% of IL; ■, 0.5 wt% of IL.

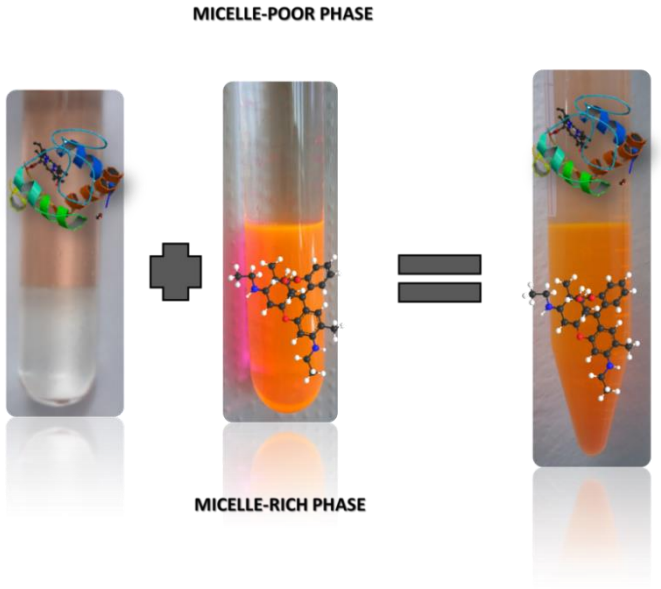

Figure 9. Illustration of the partition of Cyt c and R6G by applying the AMTPS developed in separate systems and at the same extraction systems, in a clear evidence of the selective character of this liquid-liquid extraction methodology.

2.4. CONCLUSIONS

This work studies for the first time the effect of ILs as co-surfactants on the binodal curves of AMTPS composed of Triton X-114 and the McIlvaine buffer. These results clearly demonstrate that ILs have an important effect on the T_{cloud}, *i.e.* in the binodal curves, which is highly dependent on the ILs hydrophobic/hydrophilic nature. In fact, the T_{cloud} can be considerably reduced by selecting ILs possessing a hydrophobic nature, such as those belonging to the phosphonium and quaternary ammonium families.

The extraction of two model (bio)molecules, namely the Cyt c and R6G, was carried out to evaluate the partition behavior on these systems. Cyt c is shown to be concentrated on the micelle-poor phase ($\log K_{Cyt\ c} < 0$), while R6G has an extensive migration for the opposite (micelle-rich) phase ($\log K_{Cyt\ c} > 0$). These opposite behaviors are here translated by the selectivity parameter, principally for AMTPS with ILs acting as co-surfactants. In fact, it is well demonstrated that the simple addition of a small content of these ILs has a very significant effect on improving the selective extraction of these (bio)molecules. The results herein obtained show that AMTPS with ILs as additives can be useful for the extraction and purification of (bio)molecules.

3. EXTRACTION OF THE NATURAL COLORANT CURCUMIN FROM AN OLEORESIN EXTRACT

3.1. INTRODUCTION

Over the past decade, the *Green Chemistry* concept has been intensively addressed due to the enormously amount of pollutants produced by the chemical industry and their dangers. Therefore, there has been an increased interest in environmentally friendly techniques and in the use of alternative materials such as agricultural raw materials (*85*, *86*). Curcumin is a natural colorant extracted from the turmeric *Curcuma longa* and has been used for thousands of years in the Orient as a therapeutic agent (*87–89*). Lately, this orange-yellow crystalline powder (*90*) has earned special attention owing to its wide range of applications, namely their numerous medicinal properties (anti-inflammatory (*87*, *88*, *91*, *92*), antioxidant (*87–89*, *92*), antiviral (*88*), antibacterial (*88*), antifungal (*88*) and anticancer (*87–89*, *92–94*)), neuro-protective effects against oxidative stress and as an active molecule in the Alzheimer's disease (*92*, *95*), as an amyloid-indicator dye (*96*), a dietary spice and as food colorant (*87*, *88*, *90*, *92*), a dying woven polyesters fabrics (*97*), in dye-sensitizer solar cells (*98*), etc.

The extract of *Curcuma longa* contains about 3-6% of curcuminoids (*88*, *92*), from which 50-60% corresponds to curcumin (*92*), 2-5% of essential oils and the major portion includes proteins, sugars and resins (*88*, *92*). Moreover, this colorant is stable at high temperatures and when in an acid media, being however unstable at alkaline conditions and in presence of light (*87*). On the other hand, this major curcuminoid is almost insoluble in water, log P = 4.12 (*99*), thus in order to extract and purify curcumin from the turmeric roots it is necessary to undergo different steps of extraction applying organic solvents like methanol, ethanol and acetone (*88*, *90*). Firstly, the rhizomes are cleaned, dried and grinded until there is only a powder left (*87–90*). Then, the turmeric powder is washed and treated with organic solvents so that a distillation step can be followed to evaporate one of the components (solvent or solute). The product of this step is known as oleoresin (*88*, *89*). Then, oleoresin is further exposed to several organic washings resulting in a curcumin powder (*87*, *90*). In the end of the extraction and purification process, the residues left have been proved to still have remains of this basic colorant (*90*). In addition, considering the wide range of applications previously mentioned, it is expected to have lots of wastes produced and thus, a considerable amount of curcumin that can still be extracted and used. On the other hand, there is an ecological impact to take into account since there is a substantial amount of organic solvents applied. Thereby, a new environmentally friendly approach to recover

curcumin should be pursued. AMTPS constituted by the combination of a traditional surfactant and ILs as co-surfactants emerged as a promising alternative (to substitute at least part of the steps constituting the more conventional extraction processes) being applied to the extraction of curcumin from the turmeric roots. Therefore, this work is focused on the application of these novel AMTPS as extractive technologies for the recovery of curcumin from an oleoresin extract.

3.2. EXPERIMENTAL SECTION

3.2.1. Materials

The imidazolium-based ILs, 1-decyl-3-methylimidazolium chloride [C_{10}mim]Cl (purity > 98 wt%), 1-dodecyl-3-methylimidazolium chloride [C_{12}mim]Cl (purity > 98 wt%) and 1-methyl-3-tetradecylimidazolium chloride [C_{14}mim]Cl (purity > 98 wt%) were acquired at Iolitec (Ionic Liquid Technologies, Heilbronn, Germany). All phosphonium-based ILs, namely trihexyltetradecylphosphonium chloride [$P_{6,6,6,14}$]Cl (purity = 99.0 wt%), trihexyltetradecylphosphonium bromide [$P_{6,6,6,14}$]Br (purity = 99.0 wt%), trihexyltetradecylphosphonium decanoate [$P_{6,6,6,14}$][Dec] (purity = 99 wt%) and trihexyltetradecylphosphonium bis (2,4,4-trimethylpentyl)phosphinate [$P_{6,6,6,14}$][TMPP] (purity = 93.0 wt%) were kindly offered by Cytec. The chemical structures of the cations and anions composing the list of ILs used in this particular study are depicted in **Figure 10a**. Triton X-114 (laboratory grade) was supplied by Sigma-Aldrich® and the McIlvaine buffer components, namely sodium phosphate dibasic anhydrous (Na_2HPO_4 purity ≥ 99%) and citric acid anhydrous ($C_6H_8O_7$ purity = 99.5%) were acquired at Fisher Chemical and Synth, respectively. Oleoresin extract was kindly granted by Agro-Industrial Olímpia Ltda-Brasil. The target molecule structure of this work, curcumin is presented in **Figure 10b**.

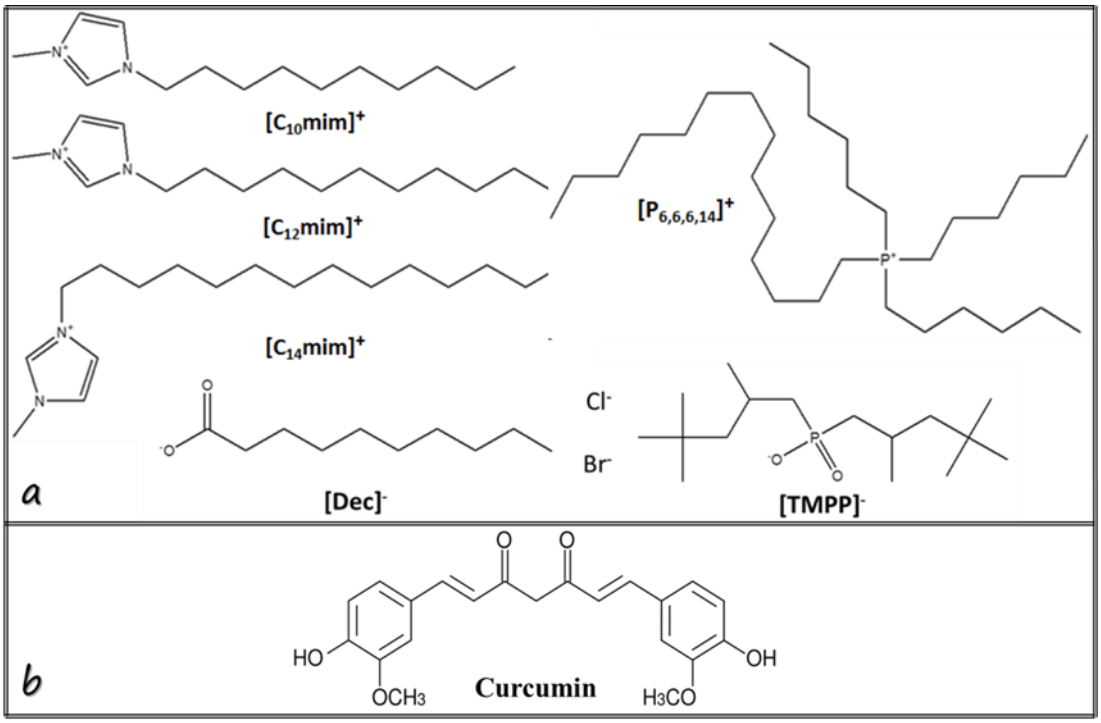

Figure 10. Chemical structure representation of the chemicals studied **a)** the cations and anions composing the ILs and **b)** curcumin.

3.2.2. Methods

3.2.2.1. Stability of Curcumin in triton X-114, ILs and McIlvaine buffer

The experiments of curcumin stability were performed in McIlvaine buffer at pH 7.0 and at 20 ± 1°C (temperature at which the solution is still clear, *i.e.* below the T_{cloud}). The pH should be maintained to guarantee the same chemical characteristics of curcumin.

For all the stability experiments, falcon tubes were weighed with 0.5 g of oleoresin extract. Afterwards, the tubes were completed with 0.25 g of Triton X -114 (10 wt%) and 1.75 g of McIlvaine buffer to perform the colorant stability tests in the surfactant; 0.0075 g of each IL (0.3 wt%) and 1.9925 g of McIlvaine buffer for the stability tests with 0.3 wt% of IL; and 0.0125 g of each $[C_n mim]Cl$, n = 10, 12, 14, (0.5 wt%) plus 1.9875 g of McIlvaine buffer for the stability studies of the natural colorant in 0.5 wt% of each IL. All systems with a final weight of 2.5 g were homogenized for approximately half an hour with a tube rotator apparatus model 270 from Fanem®, in the freezer at 7°C. Then, the systems were placed in a thermostatically controlled bath previously adjusted to 20°C. A control solution was also prepared comprising 0.5 g of curcumin extract and 2.0 g of McIlvaine buffer, exposed to the same conditions of the

previous solutions. The concentration of the dye was monitored over a 24 hour period, with samples being taken at 0, 3, 6 and 24 hours of exposure. The experiments were performed in triplicate and the respective standard deviations were determined.

The concentration of the colorant was then determined for all systems and compared with the colorant concentration calculated for the initial solution, presented in the oleoresin extract. Thus, to represent the stability of curcumin, the colorant concentration (CC) was evaluated as described in Eq. 6.

$$CC\ (\%) = \frac{CC_{sol}}{CC_{ini}}\ x\ 100 \qquad \text{(Eq. 6)}$$

where CC_{sol} stands for the colorant concentration in solution at a specific time (0, 3, 6 or 24 hours) while CC_{ini} is the inicial concentration of curcumin.

3.2.2.2. Partitioning study of curcumin using AMTPS

The binodal curves used in this work were taken from Chapter 2.

For the partitioning study of curcumin, glass tubes were weighed with specific amounts of each component: 10 wt% of Triton X-114, 0 wt%, 0.3 wt% of each IL tested or 0.5 wt% of [$C_n$mim]Cl (n = 10, 12, 14), 22.5 wt% of the oleoresin extract (including curcumin), being the McIlvaine buffer solution at pH 7 used to complete a final volume of 10 mL. The systems were homogenized for at least 2 hours in the freezer at 7 ºC, using a tube rotator apparatus model 270 from Fanem®, to avoid the turbidity of the system. Then, the systems were left at 35 ºC overnight, allowing the thermodynamic equilibrium to be reached, thus completing the separation of the phases as well as the migration of the colorant. At the conditions adopted in this work, the systems resulted in a micelle-rich and a micelle-poor, respectively, as the bottom and top layers. Both phases were carefully separated and collected for the measurement of volume, weight composition, and quantification of the colorant. The UV spectroscopy was elected to quantify each molecule at 425 nm, using a Molecular Devices Spectramax 384 Plus | UV-Vis Microplate Reader. The analytical quantifications were performed in triplicate and at least three parallel assays for each system were done, being the average values and the respective standard deviations presented. Possible interferences of the AMTPS components (Triton X-114, McIlvaine buffer or IL when present) with the analytical quantification method were prevented through routinely applying blank controls. Thus, the partition coefficient ($K_{Curcumin}$) was calculated as the ratio between the amount of

curcumin present in the micelle-rich (bottom) and the micelle-poor (top) phases, as described in Eq. 7.

$$K_{Curcumin} = \frac{[Curcumin]_{bot}}{[Curcumin]_{top}} \quad \text{(Eq. 7)}$$

where $[Curcumin]_{bot}$ and $[Curcumin]_{top}$ are, respectively, the concentration of Curcumin in the bottom and top phases. It should be mentioned that the concentration of curcumin in each phase was determined based on a calibration curve previously established.

The recovery (R) parameters of curcumin towards the bottom (R_{Bot}) and the top (R_{Top}) phases were determined following Eqs. 8 and 9:

$$R_{Bot} = \frac{100}{1+\left(\frac{1}{R_v \times K}\right)} \quad \text{(Eq. 8)}$$

$$R_{Top} = \frac{100}{1+R_v \times K} \quad \text{(Eq. 9)}$$

where R_v stands for the ratio between the volumes of the bottom and top phases.

The extraction efficiency of curcumin towards the bottom and micelle-rich phase (EE_{Bot} (%)) attained for each system was determined following the Eq. 10:

$$EE_{Bot} = \frac{m_{Bot}}{m_0} \times 100 \quad \text{(Eq. 10)}$$

where m_{Bot} and m_0 denote the mass of curcumin present in the bottom and the mass of curcumin initially added in the system, respectively.

3.3. RESULTS AND DISCUSSION

3.3.1. Stability studies

Curcumin is present in the oleoresin extract (a complex matrix) and because the ultimate application of this natural colorant is the food industry, there is an increased need to evaluate the stability of this molecule considering the system components of the AMTPS. Thus, the stability was measured to determine if any of the system agents can interfere with the colorant structure and activity, changing its native conformation. So, stability tests with the oleoresin extract were performed and the colorant concentration that resisted the studies was determined (CC) in different conditions, namely in the presence of the surfactant, or the buffer, or each one of the ILs analyzed. The results of the imidazolium family are presented in **Figure 11a**, while those belonging to the $[P_{6,6,6,14}]^+$ family are depicted in **Figure 11b**.

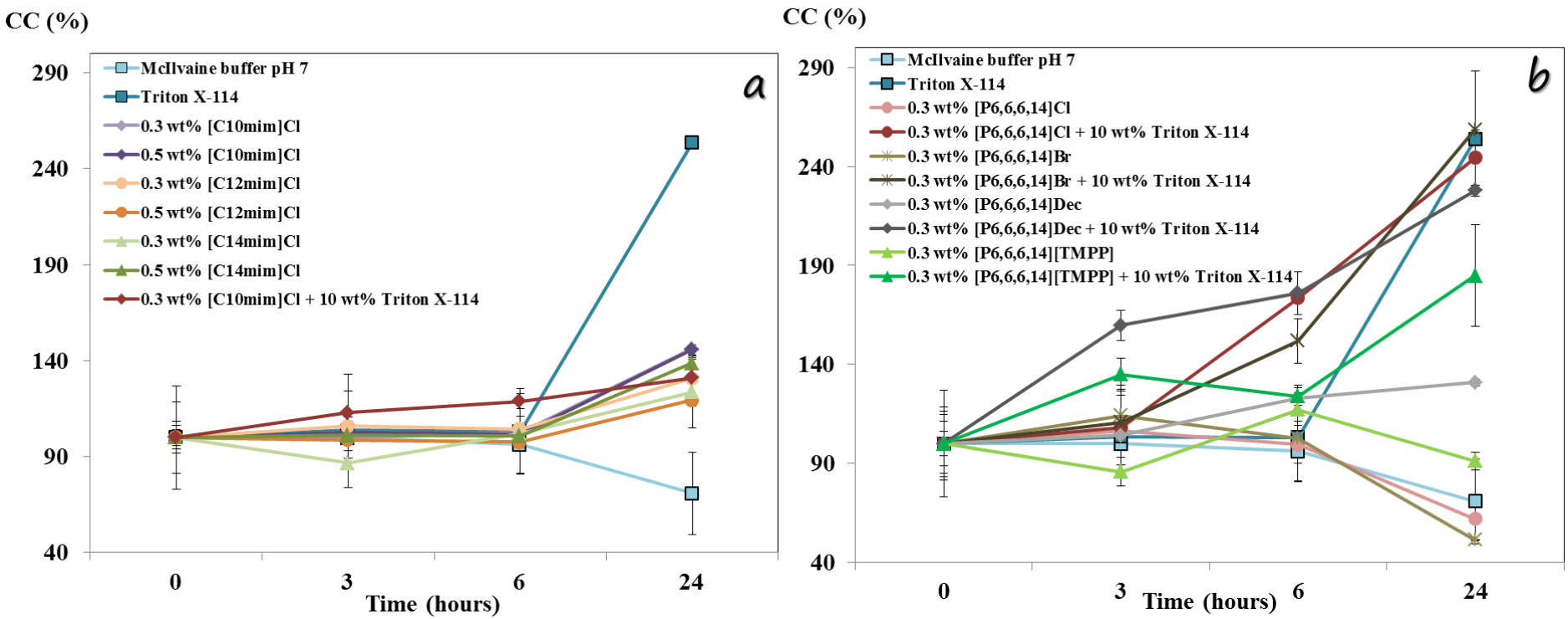

Figure 11. Stability tests of the oleoresin extract considering the colorant concentration - CC (%) - that remains after exposure to different conditions tested: the presence of only Triton X-114, McIlvaine buffer, each one of the imidazolium-based ILs (0.3 wt% and 0.5 wt%) and the phosphonium-based ILs (0.3 wt%) and then the complete AMTPS: ■, 89.7 wt% McIlvaine buffer; ■, 10 wt% Triton X-114; ♦, 0.3 wt% [C_{10}mim]Cl; ♦, 0.5 wt% [C_{10}mim]Cl; ●, 0.3 wt% [C_{12}mim]Cl; ●, 0.5 wt% [C_{12}mim]Cl; ▲, 0.3 wt% [C_{14}mim]Cl; ▲, 0.5 wt% [C_{14}mim]Cl; ♦, 0.3 wt% [C_{10}mim]Cl + 10 wt% Triton X-114 + 89.7 wt% McIlvaine buffer; ●, 0.3 wt% [$P_{6,6,6,14}$]Cl; ●, 0.3 wt% [$P_{6,6,6,14}$]Cl + 10 wt% Triton X-114 + 89.7 wt% McIlvaine buffer; ✳, 0.3 wt% [$P_{6,6,6,14}$]Br; ✳, 0.3 wt% [$P_{6,6,6,14}$]Br + 10 wt% Triton X-114 + 89.7 wt% McIlvaine buffer; ♦, 0.3 wt% [$P_{6,6,6,14}$]Dec; ♦, 0.3 wt% [$P_{6,6,6,14}$]Dec + 10 wt% Triton X-114 + 89.7 wt% McIlvaine buffer; ▲, 0.3 wt% [$P_{6,6,6,14}$][TMPP]; ▲, 0.3 wt% [$P_{6,6,6,14}$][TMPP] + 10 wt% Triton X-114 + 89.7 wt% McIlvaine buffer.

The CC for all imidazolium-based ILs as well as the CC from the surfactant and the McIlvaine buffer (**Figure 11a.**) remained constant during the first 6 hours of the study. However, after 24 hours it is clear that the interaction between curcumin and each of the ILs besides its interaction with the surfactant and the buffer. Independently of the IL used and its concentration, the IL interaction with the colorant slightly increases the CC parameter, which means that the IL may be interacting with the chromophore group, giving a small false increase in the curcumin concentration present in the extract. On the other hand, the presence of only the McIlvaine buffer seems to be negatively influencing the curcumin structure, which is here represented by a decrease in its stability after 24 hours. Moreover, when curcumin is only in contact with Triton X-114, there is a considerable increase in the CC, showing a great interaction between the surfactant and the colorant that may be compromising its integrity. In order to finalize the studies for this family, a complete system with $[C_{10}mim]Cl$ was studied as an example, and the results suggest that the presence of the IL in the whole system seems to be reducing the interaction between the surfactant and curcumin, since the final increase in the CC resembles the results obtained for the IL' presence when compared with the data obtained for the main surfactant. In this sense and taking into account the stability results, the AMTPS series based in the imidazolium family can be applied in the partitioning studies considering both concentrations, 0.3 and 0.5 wt% (details in next section 3.3.2).

As far as the phosphonium family is considered, the results (**Figure 11b.**) are not satisfactory because, apart from the $[P_{6,6,6,14}][Dec]$, all ILs are negatively interacting with the natural colorant, probably leading to irreversible alterations in its chromophore group, as can be macroscopically seen by **Figure 12**. Hence, these ILs could not be used for further partitioning studies. Nonetheless, stability tests of the complete system were done for every phosphonium chemical structure to determine the impact of the complete system in the colorant stability. In this context, it seems that Triton X-114 is strongly interacting with the colorant, turning insignificant the impact of the ILs' presence, or due to some specific interactions between the main surfactant and the colorant, which are not maintained between the colorant and the ILs, or more probably because of the greater amount of Triton X-114 used, when compared with the ILs' concentration. Thus, additional studies are required to further understand the type of interactions occurring between the colorant and each component of the system.

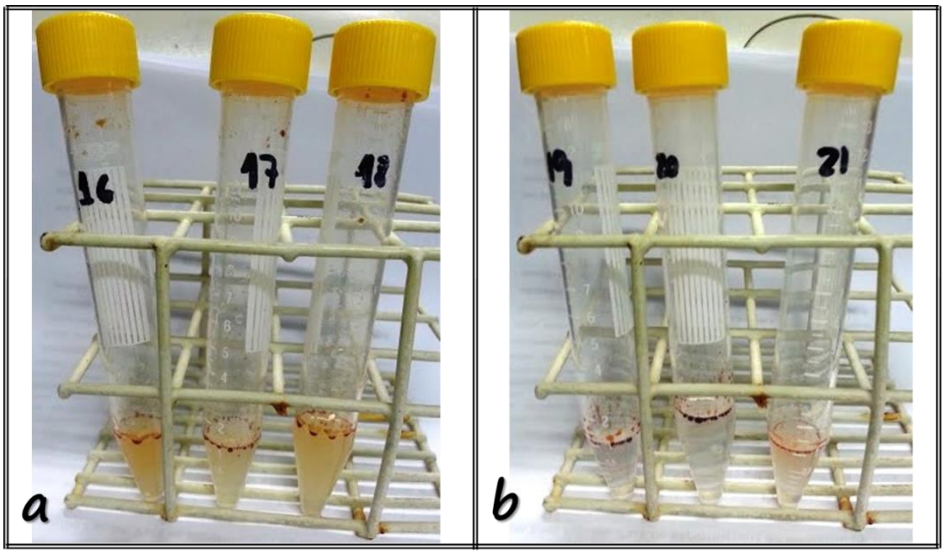

Figure 12. Macroscopic aspect of the colorant after 24 hours of exposure to **a)** $[P_{6,6,6,14}]Br$ and **b)** $[P_{6,6,6,14}]Cl$. These ILs were here used just as examples.

3.3.2. Partitioning studies of curcumin with AMTPS

In order to pursue a more environmentally friendly and sustainable approach to extract curcumin from its oleoresin extract, AMTPS composed by Triton X-114 in absence and presence of $[C_n mim]Cl$ (n = 10, 12 and 14) ILs acting as co-surfactants were investigated. In this case, and as explained before, the imidazolium family was the only capable of maintaining the stability of curcumin for a long period of time (24 hours), and thus it is the only family used in the partitioning studies. Therefore, it was possible to evaluate the influence of the IL in each system, on the partitioning of the colorant between both micelle-rich and poor phases, as well as the IL concentration. The results of the partition coefficients of curcumin, $K_{curcumin}$, are depicted in **Table 3**.

The partition studies shows that the traditional AMTPS presents the best results, $K_{curcumin}$ = 2806.46 ± 307.45, compared with the mixed AMTPS (with IL) that possess a wide range of $K_{curcumin}$ from 95.65 ± 0.29 to 2409.48 ± 342.19 correspondent to 0.3 wt% of $[C_{14}mim]Cl$ and $[C_{10}mim]Cl$, respectively. Therefore, there is an obvious tendency between the alkyl side chain of the IL which is in general, independent of the concentration, and the $K_{curcumin}$ that is the longer the alkyl chain, the lower the partition is. Albeit these EE_{Bot} are considerable increased, showing an evident interaction between the surfactant and IL with the colorant chromophore group, this tendency is also present in the EE_{Bot} for 0.3 wt% of IL, which means that an increase in the system hydrophobicity leads to a decrease in the $K_{curcumin}$.

Table 3. Presentation of results including the partition coefficients, $K_{curcumin}$, recovery (%), R_{Bot}, and extraction efficiency towards the micelle-rich phase, EE_{Bot} (%) of curcumin for $[C_n mim]Cl$ (n = 10, 12 and 14) and obtained by the application of AMTPS composed by 10 wt% Triton X-114 + McIlvaine buffer at pH 7 + different weight fraction compositions of $[C_n mim]Cl$.

Triton X-114 (wt %)	**[IL] (wt %)**	**IL**	**$K_{curcumin}$**	**R_{Bot} (%)**	**EE_{Bot} (%)**
10	0.0	---	2806.46 ± 307.45	99.93 ± 0.01	175.63 ± 5.12
	0.3	$[C_{10}mim]Cl$	2409.48 ± 342.19	99.97 ± 0.00	240.71 ± 22.89
		$[C_{12}mim]Cl$	822.84 ± 50.73	99.88 ± 0.01	133.00 ± 5.92
		$[C_{14}mim]Cl$	95.65 ± 0.29	99.00 ± 0.19	131.51 ± 5.06
	0.5	$[C_{10}mim]Cl$	60.38 ± 35.21	99,89 ± 0.06	94.99 ± 2.57
		$[C_{12}mim]Cl$	1008.92 ± 273.26	99.89 ± 0.11	96.66 ± 1.57
		$[C_{14}mim]Cl$	224.13 ± 48.65	99.80 ± 0.10	97.30 ± 2.45

These results are in agreement with those obtained by Passos *et al.* (*100*) for the extraction of bisphenol A, an organic compound such as curcumin. Moreover, within these AMTPS there are presumably two main types of interactions ruling the partitioning: hydrogen-bonding interactions and π···π interactions, accordingly to the colorant and the ILs structures. However, it is here emphasized the necessity to perform additional studies to fully understand what are the main forces driving the current interactions between the colorant and the AMTPS components, which are controlling the partition of curcumin and their structural alteration (here proved by the EE values above 100%). Right now, the only evidence presented is the complete recovery of curcumin in the micelle-rich phase of nearly 100% (**Table 3**) because these strong interactions do not allow a more detailed characterization of the systems.

3.4. CONCLUSION

From the stability tests it can be concluded that the imidazolium family is the only family of ILs studied where curcumin remains stable after 24 hours. Moreover, the surfactant has a major effect on the curcumin structure, namely with the chromophore moiety. On the other hand, the phosphonium-based ILs have a significant negative

influence in the change of the curcumin structure in such a way that can be macroscopically observed.

Furthermore, partitioning studies show a complete recovery of curcumin in the micelle-rich phase, as proved by the partition coefficients and recovery data. However, some important alterations were demonstrated in the curcumin structure when it is exposed to the AMTPS components that can only be fully understood and characterized after additional studies. Thus, is should be stressed that this work requires more evidences before it can be considered completed.

4. DEVELOPING NEW EXTRACTIVE APPROACHES FOR THE DETECTION OF TENOFOVIR DISOPROXIL FUMARATE USING AQUEOUS TWO-PHASE SYSTEMS

4.1. INTRODUCTION

Human immunodeficiency virus (HIV) is a slowly replicating virus that attacks the immunologic system, causing the acquired immunodeficiency syndrome (AIDS), which is the final stage of the disease, that leaves the organism more prone to opportunistic infections eventually leading to death (*101*). According to the Global Health Observatory (a program of the World Health Organization – WHO) 2012's report regarding the HIV/AIDS data, 35.3 million of people were living with HIV/AIDS worldwide and, only in this year AIDS derived diseases led to the death of 1.6 million people (*102*). Up to date, there is still no cure for HIV, however there are several pharmacological therapies that slower the disease's progression, thus increasing the lifespan of people with the disease. HIV/AIDS therapy is generally accomplished through the combination of three distinct antiretrovirals aiming at preventing drug-resistance or resistance to virus mutations (*103*).

Tenofovir disoproxil fumarate (TDF), a pro-drug of tenofovir, is the first member of nucleotide reverse transcriptase inhibitors. This is an oral antiretroviral which is hydrolyzed in the blood stream into tenofovir once absorbed in the intestine (*104*, *105*). Tenofovir is an adenosine monophosphate analogue, that displays an advantageous prolonged half-time (*104*, *105*). Though, because of its highly polar nature, tenofovir has a poor oral bioavailability and intestine absorption (*104*, *106*). To engender a more lipophilic nature, the strategy adopted consists on the addition of two methyl carbonate esters, promoting the increase of its octanol/water partition coefficient (log P) from -2.5 to -1.3 (*106*). Moreover, besides the improvement of oral bioavailability and intestine absorption, its stability can also be attained (*107*). Such achievements led to TDF's approval by the Food and Drug Administration (FDA) (*104*) and made it part of the antiretrovirals most used for HIV/AIDS therapy. In addition, tenofovir simply needs two additional phosphorylation reactions to be incorporated into the DNA strands, thus precluding the virus replication. This is a benefit over the remaining nucleoside analogues, which require an extra step of phosphorylation and thus, more energy and time (*104*).

Tenofovir monitoring is considered an helpful tool in the following up of HIV-infected patients, namely when there are suspicions about therapeutic non-compliance (*108*). This assessment is accomplished by determining the residual concentration of tenofovir in plasma, by different methodologies namely high-performance liquid chromatography

(HPLC) coupled with UV detection (*109–111*), HPLC coupled with tandem mass spectrometry (MS) (*108*, *112–115*), HPLC coupled with UV and MS in series (*116*) and HPLC coupled with spectrofluorimetric detection (*117*, *118*). Prior to detection assays, plasma samples are usually pre-treated either by using solid-phase extraction (SPE) cartridges (*109*, *111*, *112*, *116*) or by simply precipitating the plasma proteins using organic solvents and/or halogenated carboxylic acids (*108*, *110*, *111*, *113–115*, *117*, *118*). Yet, these methodologies are characterized by the use of hazardous substances, high cost devices and/or time consuming protocols. Moreover, SPE is sometimes problematic when attempting the separation of highly polar compounds (*119*). In fact, Reszk *et al.* (*120*) tried to comprise tenofovir in the validation of their chromatographic methodology, but they have assumed that due to the water solubility of tenofovir, it was not retained on the SPE cartridge. In this context, and since the main problem is found for aqueous environment, ATPS may be investigated as appropriate alternatives. Additionally, ATPS have been applied as pre-concentration techniques in the analytical chemistry domain. It is truly believed that they are promising alternatives to the current ones: the pre-concentration of organic pollutants from environmental samples is well-established using AMTPS (*119*); also, dodecyl sodium sulfate and an IL were used to form a suitable AMTPS for the extraction/quantification of dutasteride from human serum (*27*); polymeric ATPS were applied in the pre-treatment of water samples for the determination of a sulfonamide used in veterinary medicine with extraction efficiencies up to 100% (*121*); ATPS composed of ILs and inorganic salts successfully concentrated/extracted steroids (*122*), proteins (*123*), alkaloids (*124*) and bisphenol A (*100*) from human fluids.

In the current chapter, a novel approach to improve the assessment of TDF biodisponibility is proposed. With this aim, AMTPS composed of Triton X-114 and ILs as co-surfactants (*125*) as well as ATPS based on polymer-salt (*126*) are applied as alternative techniques for TDF extraction. The partitioning studies carried out enable the evaluation of the most adequate conditions to attain the complete extraction/concentration of TDF from the aqueous medium. After optimizing the set of conditions, it is possible to select the most appropriate systems, designing effective and sustainable techniques to detect this antiretroviral in human plasma.

4.2. EXPERIMENTAL SECTION

4.2.1. Materials

TDF (IUPAC name: ({[(2R)-1-(6-amino-9H-purin-9-yl)propan-2-yl]oxy}methyl)phosphonic acid; CAS number: 147127-20-6), was kindly supplied by Cristália and its structure is presented in **Table 4** (along with that of tenofovir).

Table 4. Chemical structures and properties presented for tenofovir and tenofovir disoproxil fumarate (TDF).

Structure	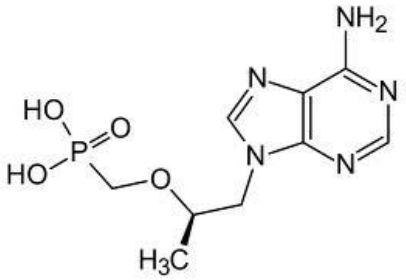 **Tenofovir**	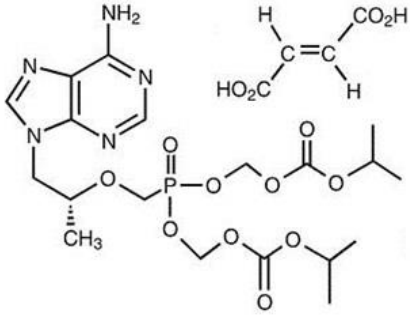 **Tenofovir disoproxil fumarate (TDF)**
Log P (*106*)	-2.5	-1.3
pK_a (*99*)	1.35; 5.12; 7.91	5.12
Water solubility (*127*)	---	13.4 $mg.mL^{-1}$

The imidazolium-based IL, 1-methyl-3-tetradecylimidazolium chloride, $[C_{14}mim]Cl$ (purity > 98 wt%), was acquired at Iolitec (Ionic Liquid Technologies, Heilbronn, Germany), while the phosphonium-based IL, trihexyltetradecylphosphonium chloride, $[P_{6,6,6,14}]Cl$ (purity = 99.0 wt%), was kindly supplied by Cytec. Triton X-114 (laboratory grade) was supplied by Sigma-Aldrich®. The chemical structures of Triton X-114 and the ILs are provided in **Figure 13a.** and **b**, respectively. The salts composing the McIlvaine's buffer at pH 7.0 were the sodium phosphate dibasic anhydrous, Na_2HPO_4 (purity ≥ 99.0%) acquired at Fisher Chemical, and the citric acid anhydrous, $C_6H_8O_7$ (purity = 99.5%) purchased at Synth. The polymer polyethylene glycol (PEG) with an average molecular weight of 600 (**Figure 13c)** was acquired at Sigma Aldrich and the salts ammonium citrate tribasic anhydrous, $(NH_4)_3C_6H_5O_7$ (purity = 100%) and sodium sulfate anhydrous, Na_2SO_4 (purity = 100%) were purchased at Synth. The sodium citrate buffer was composed by citric acid monohydrate, $C_6H_8O_7{\cdot}H_2O$ (purity = 98%) and trisodium citrate dihydrate, $Na_3C_6H_5O_7{\cdot}2H_2O$ (purity = 98%) both supplied by

Synth. The water used was purified through a Millipore Milli-Q ion-exchange system (Bedford, MA).

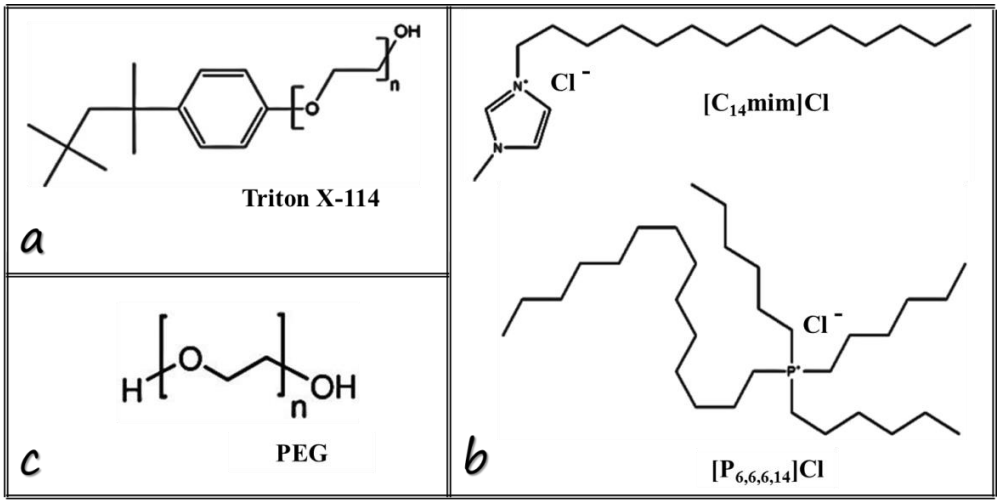

Figure 13. Chemical structure representation of **a)** the surfactant, Triton X-114, **b)** the ILs, $[C_{14}mim]Cl$ and $[P_{6,6,6,14}]Cl$ and **c)** the polymer, PEG.

4.2.2. Methods

4.2.2.1. Partitioning studies of Tenofovir using AMTPS

In order to carry out the partitioning studies of TDF using AMTPS, specific amounts of each component were weighed in glass tubes: Triton X-114 (2, 6 or 10 wt%) + IL (0, 0.3 or 0.5 wt%) + TDF solution (≈ 500 $mg.L^{-1}$) being the McIlvaine buffer solution at pH 7 (16.4 mM of Na_2HPO_4+ 1.82 mM of $C_6H_8O_7$) used to complete the final volume of the system (10 mL). The systems were homogenized (8 rpm, 7ºC, for at least 2 hours), using a tube rotator apparatus model 270 from Fanem®; then they were left at 35ºC overnight to achieve the thermodynamic equilibrium, completing the separation of the phases and the migration of TDF. At the conditions adopted in the present work, the systems gave rise to a micelle-rich and a micelle-poor as the bottom and top layers, respectively, matching the corresponding binodal curves previously determined (*125*). At the end, both phases were carefully separated and collected for characterization in terms of volume and for quantification purposes.

4.2.2.2. Partitioning studies of TDF using polymer-salt-based ATPS

The polymeric ATPS were prepared by adapting the protocol previously established by Gomes *et al.* (*126*) The appropriate amounts of PEG 600 (25 wt% or 35 wt%), of either Na_2SO_4 or $(NH_4)_3C_6H_5O_7$ (20 wt% or 30 wt%) plus an aqueous solution of TDF *at circa*

500 mg.L^{-1} (4.1 wt%) were weighed in graduated glass tubes. The sodium citrate buffer was used to complete a total weight of 10 g; the buffer was prepared by adding small amounts of $C_6H_8O_7$ (40 wt%) to $Na_3C_6H_5O_7$ (40 wt%) until the pH 6.9 was reached. The system components were homogenized in an orbital shaker (Barnstead/Thermolyne, model 400110) at 8 rpm for 30 minutes at room temperature. Then, the ATPS were placed at 35°C for at least 3 hours in order to reach the total equilibrium of the phases and migration of TDF. It should be noticed that additional experiments after 3, 5, 10 and 15 hours of rest were performed to establish the time needed to reach the equilibrium, assuring that 3 hours is enough to complete the separation (data not shown). At the end, the systems result in two clear macroscopic phases (PEG-rich and salt-rich as the top and bottom layers, respectively) with a well-defined interface in between, according to the binodal data reported elsewhere (*126*). The coexisting phases were carefully separated and collected for the quantification of the phases' volume and the antiretroviral.

4.2.2.3. Quantification of TDF and determination of the extraction parameters

The UV spectroscopy was the analytical technique selected for the quantification assays of TDF, using a Molecular Devices Spectramax 384 Plus | UV-Vis Microplate Readerat its maximum absorbance wavelength (261 nm) and employing a calibration curve previously determined. The analytical quantifications were performed in triplicate and at least three parallel assays for each system were done, being the average values and the respective standard deviations further reported. The interference of the surfactant, polymer, salts and ILs within the analytical quantification assays was investigated and excluded through the constant application of blank controls.

Two distinct parameters were determined in order to understand the partitioning phenomenon and to evaluate the extractive performance of the systems: the partition coefficient (K_{TDF}) and the extraction efficiency (EE_{TDF}) of TDF. The K_{TDF} was calculated as the ratio of the amount of TDF present in the organic phase ($[TDF]_{org}$, in mg.L^{-1}) and in the aqueous phase ($[TDF]_{aq}$, in mg.L^{-1}), according to the Eq.11:

$$K_{TDF} = \frac{[TDF]_{org}}{[TDF]_{aq}} \quad \text{(Eq. 11)}$$

The EE_{TDF} (%) attained for each system was determined following the Eq. 12:

$$EE_{TDF} = \frac{m_{org}}{m_0} \times 100 \quad \text{(Eq. 12)}$$

where m_{org} and m_0 denote the mass of TDF present in the organic phase and the mass of TDF initially added in the system, respectively.

4.3. RESULTS AND DISCUSSION

As previously mentioned, the main goal of this work is to develop a new and more effective approach for the pre-concentration of TDF to posterior quantification in plasma. Thus, AMTPS and ATPS were applied as more hydrophilic and cheaper routes for this purpose and the partitioning behavior of TDF, as well as the extractive ability of each technique was evaluated.

During the partitioning studies here reported, the effect of the AMTPS and ATPS components and compositions was evaluated while maintaining the remaining operational conditions, the pH and temperature of the medium. It is well-known that the pH of the extraction medium may have a large impact on the partitioning (*18*, *19*, *128*, *129*) process of a wide variety of molecules. Here, the AMTPS and ATPS pH media were controlled at pH 7 (McIlvaine buffer) and 6.9 (sodium citrate buffer), respectively. Thus, it is assured that the TDF remained in its neutral form (pK_a = 5.12) (*99*), avoiding the interference of additional interactions (electrostatic), beyond those naturally affecting the migration in each type of system. Also, the temperature plays an important role, especially in AMTPS (temperature dependent systems). Regardless of the temperature's minor influence on the TDF migration in conventional ATPS, it is known that it may influence the partitioning phenomenon (*130*). The temperature was thus controlled at 35ºC for both types of systems as a practical precaution and for uniformity of the data obtained. To a better understanding of all systems studied in this work using the liquid-liquid extraction methodologies and to facilitate the analysis **Table 5** was prepared.

Table 5. Types of ATPS studied and each of their components composition.

Type of ATPS	Traditional AMTPS	Novel AMTPS		PEG+Salt-based ATPS	
Triton X-114 (wt%)	2; 6; 10	10		---	
IL (wt%)	---	0.3	$[C_{14}mim]Cl$	---	
			$[P_{6,6,6,14}]Cl$	---	
PEG 600 (wt%)	---	---		25; 35	
Salt (wt%)	---	---		20; 30	Na_2SO_4
					$(NH_4)_3C_6H_5O_7$

4.3.1. Partitioning studies of TDF applying AMTPS with ILs as co-surfactants

In order to evaluate the ability of AMTPS with ILs as co-surfactants to extract TDF, distinct systems were applied: the conventional Triton X-114 + McIlvaine buffer at pH 7; and systems where ILs were included as co-surfactants: Triton X-114 + McIlvaine buffer at pH 7 + $[P_{6,6,6,14}]Cl$ or $[C_{14}mim]Cl$. Several conditions were investigated during the optimization of TDF partitioning process, namely the presence/absence of IL, as well as its structure and concentration.

The K_{TDF} and EE_{TDF} results obtained for the set of AMTPS investigated are presented in **Table 6**, evidencing that TDF presents a preferential migration towards the aqueous phase. This fact results from the TDF highly polar nature [log P = -1.3 (*106*)]. Additionally, it can be realized that the insertion of ILs as co-surfactants in AMTPS led to a decrease in TDF migration, as indicated by the reduction in the K_{TDF} values (from 0.196 ± 0.006 with the conventional AMTPS to 0.141 ± 0.003 or 0.161 ± 0.002, with 0.3 wt% of either $[P_{6,6,6,14}]Cl$ or $[C_{14}mim]Cl$, respectively, as co-surfactants). Herein, the ILs are instilling a more hydrophobic nature to the organic phase and thus, driving the TDF migration towards the aqueous phase, when compared with the common Triton X-114 micellar system.

Table 6. Partition coefficient of TDF, K_{TDF} and extraction efficiency, EE_{TDF} (%) data attained by the application of traditional and novel AMTPS composed only by Triton X-114 + McIlvaine buffer pH7 and by Triton X-114 + IL+ McIlvaine buffer pH7, respectively, at 35 ± 1ºC. The standard deviations for each parameter value are also described.

Type of ATPS	**AMTPS component concentration (wt %)**		**K_{TDF}** ± std	**EE_{TDF}** ± std **(%)**
Traditional AMTPS	Triton X-114	2	0.195 ± 0.002	2.901 ± 0.105
		6	0.205 ± 0.003	6.301 ± 0.158
		10	0.196 ± 0.006	8.027 ± 0.100
Novel AMTPS	C_{14}mimCl	0.3	0.141 ± 0.003	0.793 ± 0.022
		0.5	0.140 ± 0.006	1.082 ± 0.070
	P_{66614}Cl	0.3	0.161 ± 0.002	2.278 ± 0.055
		0.5	0.163 ± 0.004	2.055 ± 0.097

To assess the impact of the IL structure on the migration tendency of TDF, two different cations were tested, $[C_{14}mim]^+$ and $[P_{6,6,6,14}]^+$. From the results, it seems that $[C_{14}mim]Cl$, is more capable of driving the TDF towards the aqueous phase than the $[P_{6,6,6,14}]Cl$, as indicated by their lower K_{TDF} (respectively 0.141 ± 0.003 *vs* 0.161 ± 0.002 for 0.3 wt% of IL), meaning that as much closer to zero the K_{TDF}, the greater the migration of TDF is to the aqueous phase. A possible explanation for these results lies on the steric hindrance effect of the $[C_{14}mim]^+$ caused by the aromatic ring. It may prevent the approximation of TDF from its vicinity, promoting the TDF migration towards the aqueous phase (*131*). This effect has already been pointed out as one of the main interactions affecting the partitioning of (bio)molecules in ATPS (*132*). Consequently, their extractive performances are quite different, as shown by their EE_{TDF} values (**Table 6**), being a slight increase observed in the EE_{TDF} for the phosphonium family from 0.793 ± 0.022 of $[C_{14}mim]Cl$ to 2.278 ± 0.055 of $[P_{6,6,6,14}]Cl$, for 0.3 wt% of IL.

As far as the IL concentration is concerned, no clear correlation between its increase and TDF partition coefficients was noticed as the ratio between the concentrations of TDF found in both phases is constant for the systems studied, as shown in **Table 6**. Furthermore, similar results are attained for the EE_{TDF} at both concentrations of IL, since the values are quite alike with their deviation standards.

The last step in the AMTPS optimization study consisted on the use of higher concentrations of Triton X-114 (using the conventional AMTPS) aiming at generating systems with better extraction efficiencies. Again, no apparent effect of the surfactant

concentration on the partitioning of TDF (K_{TDF}) is observed. However, when increasing the surfactant concentration from 2 wt% to 10 wt%, the EE_{TDF} is enhanced from 2.901 ± 0.105 (%) up to 8.027 ± 0.100 (%).

Summing up, these AMTPS are not good pre-concentrating technologies of TDF into the organic phase, on the contrary they are great in concentrating TDF and extracting it into the aqueous phase, which is not the intended plan, since the requirement is its extraction from the human plasma, also an aqueous matrix.

4.3.2. Partitioning studies of TDF applying ATPS based on PEG 600-salt

Aiming at evaluating the performance of PEG 600-salt ATPS in the extraction of TDF, several partitioning studies were conducted using systems based in PEG 600 + $(NH_4)_3C_6H_5O_7$ + sodium citrate buffer at pH 6.9 and PEG 600 + Na_2SO_4 + sodium citrate buffer at pH 6.9. In this step of optimization, the influence of the salt nature (inorganic *vs.* organic), the salt concentration (from 20 wt% to 30 wt%), as well as the amount of PEG 600 were evaluated. The importance of applying organic salts, such as citrates, lies on the minimization of environmental concerns related with the technology. Indeed, the application of ATPS composed of inorganic salts represents a disadvantage related with their disposal into effluent streams, leading to environmental issues (*11*); the use of organic salts instead, enables the direct discharge into biological treatment plants, since they are biodegradable and non-toxic (*11*). PEG 600 was here applied due to its physical-chemical stability, low cost, low viscosity and negligible toxicity (*12*). The results obtained for the migration of the retroviral compound are depicted in **Table 7**. Those results suggest the preferential migration of TDF to the organic phase, independently of the salt used. This fact is supported by the capacity of the salt to act as the "salting-out" agent, thus forcing the migration of TDF towards the organic phase.

In what regards the salt concentration effect [considering either the Na_2SO_4 or the $(NH_4)_3C_6H_5O_7$] no significant effects are noticed in either K_{TDF} or EE_{TDF} values. For instance, the increase in Na_2SO_4 concentration led to similar K_{TDF} values of 6.103 ± 0.173 and 6.238 ± 0.044, as well as comparable EE_{TDF} of 100.000 ± 2.177 % and 96.116 ± 1.866 % (25 wt% of PEG 600 + 20 and 30 wt% of Na_2SO_4, respectively). However,

the scenario completely changes when the nature of the salt is tested: if in one hand the organic salt showed analogous K_{TDF} to those obtained with Na_2SO_4 (6.103 ± 0.173 *vs.* 6.095 ± 0.017 *at ca.* 25 wt% of PEG 600 and 6.161 ± 0.172 *at ca.* 35 wt% of PEG 600, respectively), on the other hand, the $(NH_4)_3C_6H_5O_7$ addition was followed by a decline in the EE_{TDF}, of around 20 % (*e.g.* EE_{TDF} for the mixture point 25 wt% of PEG 600 and 20 wt% of Na_2SO_4 or $(NH_4)_3C_6H_5O_7$ are 100.000 ± 2.177 and 79.506 ± 4.293 (%), respectively). Though, this salt nature effect can be easily minimized by increasing the amount of polymer from 25 wt% to 35 wt% in the systems with higher amount of $(NH_4)_3C_6H_5O_7$ (EE_{TDF} = 91.239 ± 2.388 %). Nonetheless, the impact of PEG 600 concentration on the TDF migration was generally negligible, concerning both K_{TDF} and EE_{TDF} (**Table 7**).

Table 7. Partition coefficient of TDF, K_{TDF} and extraction efficiency, EE_{TDF} (%) data obtained by the application of ATPS composed of PEG 600 at different weight fraction compositions + Na_2SO_4 or $(NH_4)_3C_6H_8O_7$ at distinct weight fraction compositions + sodium citrate buffer pH 6.9, at 35 ± 1ºC.

System composition		K_{TDF}	EE_{TDF} (%)
25 wt% PEG	**20 wt% Na_2SO_4**	6.103 ± 0.173	100.000 ± 2.177
	30 wt% Na_2SO_4	6.238 ± 0.044	96.116 ± 1.866
35 wt% PEG	**20 wt% Na_2SO_4**	6.914 ± 0.108	98.817 ± 3.610
	30 wt% Na_2SO_4	6.936 ± 0.044	99.547 ± 2.544
25 wt% PEG	**20 wt% $(NH_4)_3C_6H_5O_7$**	6.095 ± 0.017	79.506 ± 4.293
	30 wt% $(NH_4)_3C_6H_5O_7$	6.204 ± 0.262	74.399 ± 4.362
35 wt% PEG	**20 wt% $(NH_4)_3C_6H_5O_7$**	6.161 ± 0.172	84.187 ± 2.110
	30 wt% $(NH_4)_3C_6H_5O_7$	6.555 ± 0.333	91.239 ± 2.388

4.3.3. Development of sustainable technologies for the extraction/concentration of TDF

Considering the optimization studies carried out, where several parameters of both AMTPS and ATPS have been optimized, it is possible now to compare the various systems and provide an overview of the results. At this moment, the optimal systems can be ranked, according to their extractive performance (EE_{TDF}), as follows:

PEG 600 + Na_2SO_4 + sodium citrate buffer at pH 6.9 > PEG 600 + $(NH_4)_3C_6H_5O_7$ + sodium citrate buffer at pH 6.9 > Triton X-114 + McIlvaine buffer at pH 7 >

Triton X-114 + McIlvaine buffer at pH 7 + $[P_{6,6,6,14}]Cl$ > Triton X-114 + McIlvaine buffer at pH 7 + $[C_{14}mim]Cl$.

It should be emphasized that the concentrations of IL, Triton X-114, PEG 600 and salts considered in the tendency previously shown are those allowing the highest EE_{TDF} attainable by each system. However, the results attained for the AMTPS from now on are not being considered due to their poor ability to concentrate the TDF in the organic phase. On the other hand, the ATPS values are remarkable and generally higher to those obtained using the current techniques. For instance, the performance of SPE in the extraction of tenofovir from plasma was unconvincing according to the main conclusions found in literature, the values varying from its complete incapability (*120*), passing through intermediate performances around 64% (*109*) up to complete extraction (*111*, *116*). The same scenario is observed when the extraction is accomplished by means of protein precipitation (*113*, *114*). Besides, and as aforementioned, these ATPS provide relevant economic and environmental issues, related with the experimental design required (including time needs and cost of the apparatus and materials). Indeed, ATPS delivered an efficient technique based not only on the partition, but also by the extraction parameters achieved (K_{TDF} and/or EE_{TDF}), while maintaining a sustainable profile of the whole methodology. Moreover, the substitution of the inorganic Na_2SO_4 by the biodegradable $(NH_4)_3C_6H_5O_7$ salt in the creation of polymeric ATPS, allowed the development of a greener strategy, keeping the (complete) extractive ability.

Although TDF was applied during the partitioning studies, it is possible to anticipate that the systems would remain applicable in the case of tenofovir (more hydrophilic nature, **Table 4**). In this sense, it was possible to strategically design distinct sustainable approaches to be applied in the extraction/concentration of TDF and tenofovir in human plasma.

4.4. CONCLUSION

This work introduces a new alternative for TDF pre-concentration, namely the PEG 600-salt-based ATPS, to be applied in the field of analytical chemistry. The optimization studies evidenced the high operational versatility and simplicity of such techniques. The complete concentration of TDF in one phase was easily achieved, by optimizing a few operational parameters, namely the amount or chemical nature of the

phase forming agents. The AMTPS, both the conventional and the novel ones showed poor ability to concentrate and extract TDF in the organic phase. Nevertheless, the polymeric ATPS displayed remarkable results. After fine-tuning both salt and PEG 600 concentrations, it was possible to substitute the inorganic Na_2SO_4 (EE_{TDF} = 100 %) by a more benign salt, the organic $(NH_4)_3C_6H_5O_7$ (EE_{TDF} = 91.2 ± 2.4 %) without compromising the performance of the process. These results indicate that these ATPS are promising candidates to substitute the current techniques used in the extraction/concentration of TDF. This fact is based not only on the high extractive performances attained, but also on a sustainable point of view: these ATPS are fast and simple techniques that do not make use of environmentally nefarious chemicals or expensive devices. It should be stressed that these systems may be compatible with the use of HPLC (combined with any type of detector, *e.g.* UV and MS), which is the technique commonly used for the reliable determination of tenofovir in plasma; an usual combination (*27*, *133–135*) for analytical purposes.

5. FINAL REMARKS, ONGOING WORKS AND FUTURE PERSPECTIVES

5.1. GENERAL CONCLUSIONS

Herein, it is presented for the first time the coexistence curves of AMTPS composed by the nonionic surfactant Triton X-114 and three distinct families of ILs acting as co-surfactants. Several effects on the T_{cloud} were evaluated such as the absence/presence of the IL, its concentration and its structural features. These novel systems were then applied to Cyt c and R6G (here used as model (bio)molecules), in which it was clear a boost in their extractive parameters, namely their partition coefficient and selectivity. Afterwards, some of these AMTPS were used in two different approaches: extraction of a natural colorant curcumin from its vegetal extract with a complete recovery of the colorant into the micelle-rich phase but with strong, and yet unknown, interactions which are affecting the colorant chemical structure; and the quantitative determination of TDF into the analytical chemistry field with extractive efficiencies of nearly 100 %, presenting a new and more sustainable approach than those being applied nowadays.

5.2. ONGOING WORK AND FUTURE PERSPECTIVES

Two different perspectives can be considered while continuing the study of AMTPS using ILs as co-surfactants. The first regards their application as extractive processes: they can be applied to a plethora of compounds from different types of matrices, they may overcome the problems displayed by the current technologies for some (bio)molecules of interest. The second approach is related with the mechanisms governing the micelle formation and structure characterization, as well as bringing new possible combinations of phase forming agents. In this context, small-angle X-ray scattering (SAXS) measurements have already started and are being performed in order to provide deeper insights into the shape, size and distribution of the micelles. This work is being developed in a close collaboration with Prof. Dr. Leandro Barbosa, Faculdade de Física - Universidade de São Paulo. Additional efforts will be done to understand not only the formation and structure of the micelles, but also the main interactions governing the phase formation phenomenon through surface and fluorescence measurements, as well as NMR studies (*136, 137*). This knowledge is of utmost importance in the selection of the AMTPS and consequently, in the creation of more efficient technologies. Besides the molecular-level studies, new AMTPS employing cationic and anionic surfactants should also be studied in conjugation with

ILs (as co-surfactants). This manipulation of the surfactant's properties may be useful to create more performant and selective systems for certain (bio)molecules and applications (*54*).

5.2.1. Norbixin extraction

Following the same line of research of that described in CHAPTER 3, the extraction of norbixin, a natural colorant from urucum will be performed. The importance of this project lies on the diverse applications of norbixin, namely as food colorant (*138*, *139*) and pharmaceutical vehicle (*140*), as well as its antioxidant properties and DNA protection (*141*). Moreover, norbixin has an important ecological role, since it is abundant in Brazil, Peru and Quenia (*139*). Unlike curcumin, this colorant is only stable at alkaline pH, so binodal curves at higher pH values are required. The determination of the binodal curves using a sodium carbonate-bicarbonate buffer at pH 10 (**Figure 14**) was already started, allowing the evaluation of the buffer influence on the T_{cloud}.

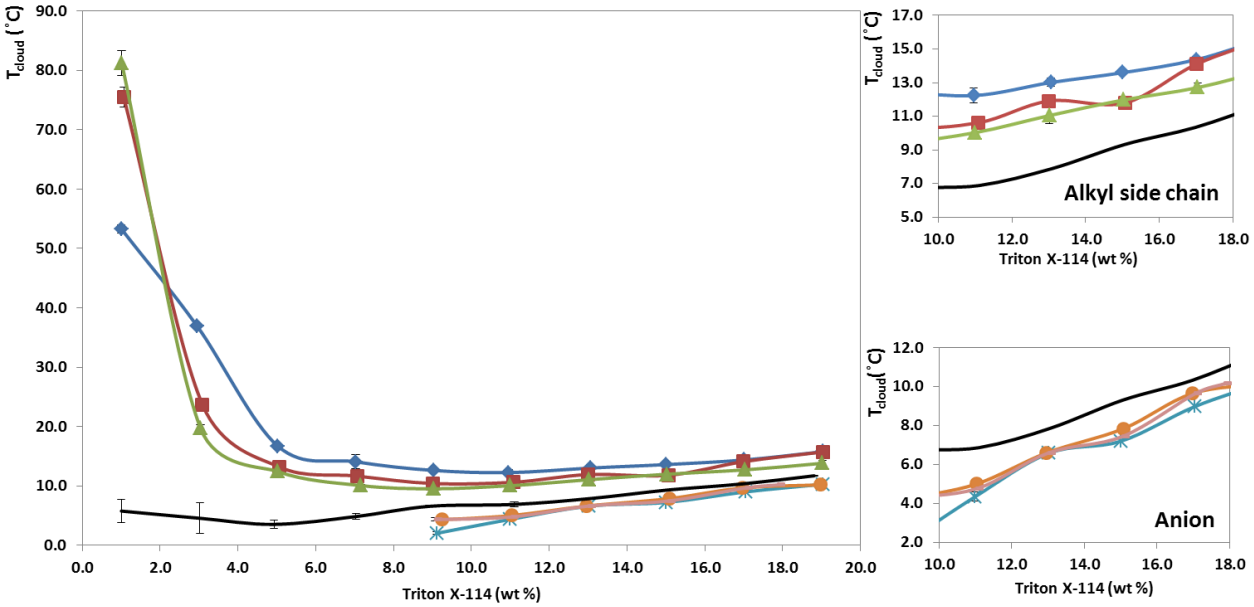

Figure 14. Binodal curves for the studied ILs at 0.3 wt% and pH 10: —, without IL; ◆, [C_{10}mim]Cl; ■, [C_{12}mim]Cl; ▲, [C_{14}mim]Cl; ✳, [$P_{6,6,6,14}$]Br; ●, [$P_{6,6,6,14}$][Dec]; □, [$P_{6,6,6,14}$][TMPP]; The effect of ILs' structural features is provided separately in the insets to facilitate the analysis.

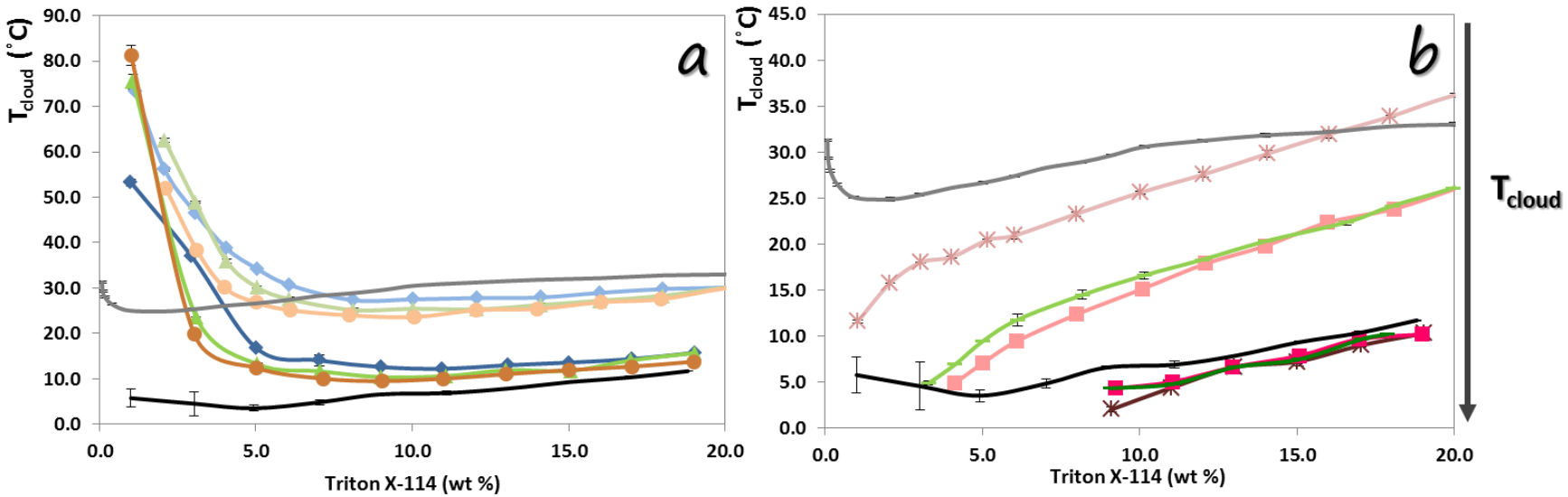

Figure 15. Effect of the pH on the T_{cloud} for all the studied ILs, at 0.3 wt%. In **a)** is presented the effect on the imidazolium family: —, without IL at pH 7; —, without IL at pH 10; ◆, [C_{10}mim]Cl at pH 7; ◆, [C_{10}mim]Cl at pH 10; ▲, [C_{12}mim]Cl at pH 7; ▲, [C_{12}mim]Cl at pH 10; ●, [C_{14}mim]Cl at pH 7; ●, [C_{14}mim]Cl at pH 10; and in **b)** is presented the effect on the phosphonium family: ✳, [$P_{6,6,6,14}$]Br at pH 7; ✳, [$P_{6,6,6,14}$]Br at pH 10; ■, [$P_{6,6,6,14}$][Dec] at pH 7; ■, [$P_{6,6,6,14}$][Dec] at pH 10; -, [$P_{6,6,6,14}$][TMPP] at pH 7; -, [$P_{6,6,6,14}$][TMPP] at pH 10.

The binodal curves (**Figure 14 and 15**) denote the same tendency on the AMTPS containing [$C_n$mim]Cl as that previously discussed, *i.e.* the T_{cloud} increases as the alkyl side chain of the IL decreases. On the other hand, at this pH the effect of the phosphonium-based IL anions is negligible, probably due to a superposition of the effect related with the strong basicity of the buffer. It is clear that the pH has a huge effect on the T_{cloud} of both types of AMTPS (with and without IL); for instance, the AMTPS possessing [$C_n$mim]Cl, n = 10, 12 and 14, and [$P_{6,6,6,14}$]Br presented a significant decrease in the T_{cloud} of more than 10 ˚C. This fact is in accordance to the evidences found for the impact of the addition of electrolytes on the T_{cloud} (*45*).

5.2.2. LDL⁻ scFv antibody extraction

Furthermore, preliminary studies were performed to apply the AMTPS with and without ILs at pH 7 to the extraction of biopharmaceuticals, namely the single chain variable fragment (scFv) antibody against electronegative low density lipoprotein (LDL^-) (produced by *Pichia pastoris*). Still, there is no accurate methodology to purify the LDL^- scFv antibody from its fermented broth. There are evidences concerning both scFv stability in surfactant-based medium (*142*) and extraction from its fermented broth using conventional AMTPS (*143*). Since these new AMTPS composed by Triton X-114 and ILs as co-surfactants showed enhanced performances, they may be envisaged as enhanced routes for the extraction of this LDL^- scFv antibody. Malpiedi and co-workers (*143*) reported significant decreases in the T_{cloud} (*circa* 10˚C) caused by the presence of the fermented broth, and following these evidences, this work was started by studies concerning the effect of the fermented broth on the binodal curves of AMTPS (**Figure 16)**.

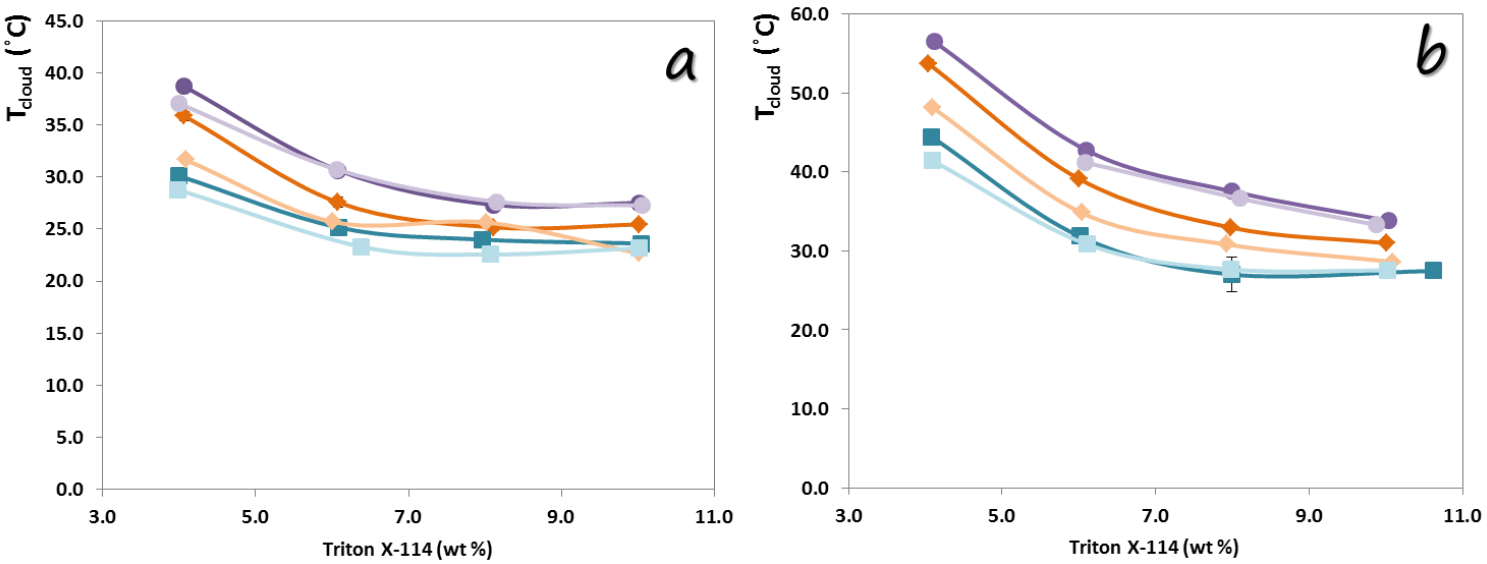

Figure 16. Effect of the fermented broth on the T_{cloud} for the imidazolium family. In **a)** and **b)** it is presented the effect of 0.3% wt and 0.5% wt of IL, respectively : ●, [C_{10}mim]Cl without fermented broth; ●, [C_{10}mim]Cl with fermented broth; ♦, [C_{12}mim]Cl without fermented broth; ♦, [C_{12}mim]Cl m with fermented broth; ■, [C_{14}mim]Cl without fermented broth; ■, [C_{14}mim]Cl with fermented broth.

From **Figure 16**, it is possible to conclude that the fermented broth is not responsible for a significant effect on the T_{cloud}. The differences noted between these results and those attained by Malpiedi *et al.*(*143*) are probably explained by the improvements done during the fermentation step. Since the production of LDL^- scFv antibody fragment is quite recent, several steps through the upstream and downstream processes are still under optimization. The next step in this work will comprise several stability tests, the validation of the partitioning studies by applying this new class of AMTPS and the study of different conditions towards the extraction performance.

5.2.3. Bromelain extraction

As future work, it was already proposed to study the application of AMTPS with ILs as co-surfactants to enhance the extraction of bromelain, a mixture of proteolytic enzymes, from pineapples due to its wide range of therapeutic benefits, such as reversible inhibition of platelet aggregation, prevention and minimization of cardiovascular diseases, action as adjuvant therapeutic agents in chronic inflammatory and autoimmune diseases, action as food supplements, among others (*144*). Beyond its high added-value, bromelain is present in high abundance in the stem and peel of pineapples and thus, it is a waste inexpensive bioproduct (*144*). In this particular approach, no preliminary studies have yet been performed.

5.3. LIST OF PUBLICATIONS

- Jorge F.B. Pereira; Filipa Vicente; Valéria C. Santos-Ebinuma; Janete M. Araújo; Adalberto Pessoa; Mara G. Freire, João A.P. Coutinho, "Extraction of tetracycline from fermentation broth using aqueous two-phase systems composed of polyethylene glycol and cholinium-based salts", Process Biochemistry, April 2013, volume 48, issue 4, pages 716–722.
- Filipa A. Vicente; Luciana P. Malpiedi; Francisca A. e Silva; Adalberto Pessoa Jr.; João A. P. Coutinho; Sónia P. M. Ventura, "Design of novel aqueous micellar two-phase systems using ionic liquids as co-surfactants for the selective extraction of (bio)molecules", Separation and Purification Technology, accepted.
- Filipa A. Vicente; André Moreni Lopes; Camila de Oliveira Melo; Francisca A. e Silva; Sónia P. M. Ventura; Adalberto Pessoa-Jr; José Alexsandro da Silva,

"Developing extractive approaches for the detection of tenofovir disoproxilfumarate using aqueous two-phase systems", in preparation.

5.4. COMMUNICATIONS

- Pereira, Jorge F. B.; Vicente, Filipa; Santos-Ebinuma, Valéria C.; Araújo, Janete M.; Pessoa Jr, Adalberto; Freire, Mara G.; Coutinho, João A. P., "Extraction of Tetracycline from Fermentation Broth using Aqueous Biphasic Systems composed of Polyethylene Glycol and Cholinium-based Ionic Liquids"; 5th Congress on Ionic Liquids (COIL-5), Algarve, Portugal, April 2013.
- Filipa A. Vicente; Luciana P. Malpiedi; Francisca A. e Silva; Adalberto Pessoa Jr.; João A. P. Coutinho; Sónia P. M. Ventura, "Micellar Extraction using Ionic Liquids as Co-Surfactants", accepted for a poster presentation at 2nd International Conference on Ionic Liquids in Separation and Purification Technology (ILSEPT).
- Filipa A. Vicente; Luciana P. Malpiedi; Francisca A. e Silva; Adalberto Pessoa Jr.; João A. P. Coutinho; Sónia P. M. Ventura, "Selective Extraction of (Bio)molecules by Applying Novel Aqueous Micellar Two-Phase Systems Composed of Triton X-114 and Ionic Liquids as Co-surfactants", accepted for a poster presentation at Chempor 2014, Porto.

6. REFERENCES

(1) Langer, E. Trends in Downstream Bioprocessing. *BioPharm Int.* **2013**, *26*, 32–36.
(2) Gottschalk, U. Bioseparation in Antibody Manufacturing: The Good, The Bad and The Ugly. *Biotechnol. Prog.* **2008**, *24*, 496–503.
(3) Mazzola, P. G.; Lopes, A. M.; Hasmann, F. A.; Jozala, A. F.; Penna, T. C. V; Magalhaes, P. O.; Rangel-Yagui, C. O.; Pessoa Jr, A. Liquid–liquid extraction of biomolecules: an overview and update of the main techniques. *J. Chem. Technol. Biotechnol.* **2008**, *83*, 143–157.
(4) Molino, J. V. D.; Viana Marques, D. de A.; Júnior, A. P.; Mazzola, P. G.; Gatti, M. S. V. Different types of aqueous two-phase systems for biomolecule and bioparticle extraction and purification. *Biotechnol. Prog.* **2013**, *29*, 1343–1353.
(5) Martínez-Aragón, M.; Burghoff, S.; Goetheer, E. L. V; de Haan, A. B. Guidelines for solvent selection for carrier mediated extraction of proteins. *Sep. Purif. Technol.* **2009**, *65*, 65–72.
(6) Asenjo, J. A.; Andrews, B. A. Aqueous two-phase systems for protein separation: A perspective. *J. Chromatogr. A* **2011**, *1218*, 8826–8835.
(7) Da Silva, L. .; Meirelles, A. . Phase equilibrium in polyethylene glycol/maltodextrin aqueous two-phase systems. *Carbohydr. Polym.* **2000**, *42*, 273–278.
(8) Rito-Palomares, M.; Negrete, A.; Miranda, L.; Flores, C.; Galindo, E.; Serrano-Carreón, L. The potential application of aqueous two-phase systems for in situ recovery of 6-pentyl-∞-pyrone produced by Trichoderma harzianum. *Enzyme Microb. Technol.* **2001**, *28*, 625–631.
(9) Bridges, N. J.; Gutowski, K. E.; Rogers, R. D. Investigation of aqueous biphasic systems formed from solutions of chaotropic salts with kosmotropic salts (salt-salt ABS). *Green Chem.* **2007**, *9*, 177–183.
(10) Lima, Á. S.; Alegre, R. M.; Meirelles, A. J. A. Partitioning of pectinolytic enzymes in polyethylene glycol/potassium phosphate aqueous two-phase systems. *Carbohydr. Polym.* **2002**, *50*, 63–68.
(11) Zafarani-Moattar, M. T.; Sadeghi, R.; Hamidi, A. A. Liquid–liquid equilibria of an aqueous two-phase system containing polyethylene glycol and sodium citrate: experiment and correlation. *Fluid Phase Equilib.* **2004**, *219*, 149–155.
(12) Liu, Y.; Yu, Y. L.; Chen, M. Z.; Xiao, X. Advances in Aqueous Two-Phase Systems and Applications in Protein Separation and Purification. *Can. J. Chem. Eng. Technol.* **2011**, *Vol. 2*, *No*.
(13) Freire, M. G.; Pereira, J. F. B.; Francisco, M.; Rodríguez, H.; Rebelo, L. P. N.; Rogers, R. D.; Coutinho, J. A. P. Insight into the Interactions That Control the Phase Behaviour of New Aqueous Biphasic Systems Composed of Polyethylene Glycol Polymers and Ionic Liquids. *Chem. – A Eur. J.* **2012**, *18*, 1831–1839.
(14) Freire, M. G.; Cláudio, A. F. M.; Araújo, J. M. M.; Coutinho, J. A. P.; Marrucho, I. M.; Canongia Lopes, J. N.; Rebelo, L. P. N. Aqueous biphasic systems: a boost brought about by using ionic liquids. *Chem. Soc. Rev.* **2012**, *41*, 4966–95.
(15) Brennecke, J. F.; Maginn, E. J. Ionic liquids: Innovative fluids for chemical processing. *AIChE J.* **2001**, *47*, 2384–2389.
(16) Aparicio, S.; Atilhan, M.; Karadas, F. Thermophysical Properties of Pure Ionic Liquids: Review of Present Situation. *Ind. Eng. Chem. Res.* **2010**, *49*, 9580–9595.
(17) Gutowski, K. E.; Broker, G. A.; Willauer, H. D.; Huddleston, J. G.; Swatloski, R. P.; Holbrey, J. D.; Rogers, R. D. Controlling the Aqueous Miscibility of Ionic Liquids: Aqueous Biphasic Systems of Water-Miscible Ionic Liquids and Water-

Structuring Salts for Recycle, Metathesis, and Separations. *J. Am. Chem. Soc.* **2003**, *125*, 6632–6633.
(18) e Silva, F. A.; Sintra, T.; Ventura, S. P. M.; Coutinho, J. A. P. Recovery of paracetamol from pharmaceutical wastes. *Sep. Purif. Technol.* **2014**, *122*, 315–322.
(19) Pereira, J. F. B.; Vicente, F.; Santos-Ebinuma, V. C.; Araújo, J. M.; Pessoa, A.; Freire, M. G.; Coutinho, J. A. P. Extraction of tetracycline from fermentation broth using aqueous two-phase systems composed of polyethylene glycol and cholinium-based salts. *Process Biochem.* **2013**, *48*, 716–722.
(20) Shahriari, S.; Tome, L. C.; Araujo, J. M. M.; Rebelo, L. P. N.; Coutinho, J. A. P.; Marrucho, I. M.; Freire, M. G. Aqueous biphasic systems: a benign route using cholinium-based ionic liquids. *RSC Adv.* **2013**, *3*, 1835–1843.
(21) Passos, H.; Ferreira, A. R.; Cláudio, A. F. M.; Coutinho, J. A. P.; Freire, M. G. Characterization of aqueous biphasic systems composed of ionic liquids and a citrate-based biodegradable salt. *Biochem. Eng. J.* **2012**, *67*, 68–76.
(22) Domínguez-Pérez, M.; Tomé, L. I. N.; Freire, M. G.; Marrucho, I. M.; Cabeza, O.; Coutinho, J. A. P. (Extraction of biomolecules using) aqueous biphasic systems formed by ionic liquids and aminoacids. *Sep. Purif. Technol.* **2010**, *72*, 85–91.
(23) Freire, M. G.; Louros, C. L. S.; Rebelo, L. P. N.; Coutinho, J. A. P. Aqueous biphasic systems composed of a water-stable ionic liquid + carbohydrates and their applications. *Green Chem.* **2011**, *13*, 1536–1545.
(24) Pereira, J. F. B.; Ventura, S. P. M.; e Silva, F. A.; Shahriari, S.; Freire, M. G.; Coutinho, J. A. P. Aqueous biphasic systems composed of ionic liquids and polymers: A platform for the purification of biomolecules. *Sep. Purif. Technol.* **2013**, *113*, 83–89.
(25) Pereira, J. F. B.; Rebelo, L. P. N.; Rogers, R. D.; Coutinho, J. A. P.; Freire, M. G. Combining ionic liquids and polyethylene glycols to boost the hydrophobic-hydrophilic range of aqueous biphasic systems. *Phys. Chem. Chem. Phys.* **2013**, *15*, 19580–19583.
(26) Bhatt, D.; Maheria, K.; Parikh, J. Studies on Surfactant–Ionic Liquid Interaction on Clouding Behaviour and Evaluation of Thermodynamic Parameters. *J. Surfactants Deterg.* **2013**, *16*, 547–557.
(27) Gong, A.; Zhu, X. Surfactant/ionic liquid aqueous two-phase system extraction coupled with spectrofluorimetry for the determination of dutasteride in pharmaceutical formulation and biological samples. *Fluid Phase Equilib.* **2014**, *374*, 70–78.
(28) Liu, J.; Jiang, G.; Jönsson, J. Å. Application of ionic liquids in analytical chemistry. *TrAC Trends Anal. Chem.* **2005**, *24*, 20–27.
(29) Sun, P.; Armstrong, D. W. Ionic liquids in analytical chemistry. *Anal. Chim. Acta* **2010**, *661*, 1–16.
(30) Soukup-Hein, R. J.; Warnke, M. M.; Armstrong, D. W. Ionic Liquids in Analytical Chemistry. *Annu. Rev. Anal. Chem.* **2009**, *2*, 145–168.
(31) Ho, T. D.; Zhang, C.; Hantao, L. W.; Anderson, J. L. Ionic Liquids in Analytical Chemistry: Fundamentals, Advances, and Perspectives. *Anal. Chem.* **2013**, *86*, 262–285.
(32) Hoogerstraete, T. Vander; Onghena, B.; Binnemans, K. Homogeneous Liquid–Liquid Extraction of Metal Ions with a Functionalized Ionic Liquid. *J. Phys. Chem. Lett.* **2013**, *4*, 1659–1663.

(33) Domańska, U.; Rękawek, A. Extraction of Metal Ions from Aqueous Solutions Using Imidazolium Based Ionic Liquids. *J. Solution Chem.* **2009**, *38*, 739–751.
(34) Wei, G.-T.; Chen, J.-C.; Yang, Z. Studies on Liquid/liquid Extraction of Copper Ion with Room Temperature Ionic Liquid. *J. Chinese Chem. Soc.* **2003**, *50*, 1123–1130.
(35) Fischer, L.; Falta, T.; Koellensperger, G.; Stojanovic, A.; Kogelnig, D.; Galanski, M.; Krachler, R.; Keppler, B. K.; Hann, S. Ionic liquids for extraction of metals and metal containing compounds from communal and industrial waste water. *Water Res.* **2011**, *45*, 4601–4614.
(36) Ni, X.; Xing, H.; Yang, Q.; Wang, J.; Su, B.; Bao, Z.; Yang, Y.; Ren, Q. Selective Liquid–Liquid Extraction of Natural Phenolic Compounds Using Amino Acid Ionic Liquids: A Case of α-Tocopherol and Methyl Linoleate Separation. *Ind. Eng. Chem. Res.* **2012**, *51*, 6480–6488.
(37) Liu, J.; Jiang, G.; Chi, Y.; Cai, Y.; Zhou, Q.; Hu, J.-T. Use of Ionic Liquids for Liquid-Phase Microextraction of Polycyclic Aromatic Hydrocarbons. *Anal. Chem.* **2003**, *75*, 5870–5876.
(38) Sarafraz-Yazdi, A.; Vatani, H. A solid phase microextraction coating based on ionic liquid sol–gel technique for determination of benzene, toluene, ethylbenzene and o-xylene in water samples using gas chromatography flame ionization detector. *J. Chromatogr. A* **2013**, *1300*, 104–111.
(39) Liu, C.; Kamei, D. T.; King, J. A.; Wang, D. I. C.; Blankschtein, D. Separation of proteins and viruses using two-phase aqueous micellar systems. *J. Chromatogr. B Biomed. Sci. Appl.* **1998**, *711*, 127–138.
(40) Liu, C.-L.; Nikas, Y. J.; Blankschtein, D. Novel bioseparations using two-phase aqueous micellar systems. *Biotechnol. Bioeng.* **1996**, *52*, 185–192.
(41) Rangel-Yagui, C. O.; Pessoa-Jr, A.; Blankschtein, D. Two-phase aqueous micellar systems: an alternative method for protein purification. *Brazilian J. Chem. Eng.* **2004**, *21*, 531–544.
(42) Tani, H.; Kamidate, T.; Watanabe, H. Aqueous Micellar Two-Phase Systems for Protein Separation. *Japan Soc. Anal. Chem.* **1998**, *14*, 875–888.
(43) Tuteja, R.; Kaushik, N.; Kaushik, C. P.; Sharma, J. K. Recovery of Reactive (Triazine) Dyes from Textile Effluent by Solvent Extraction Process. *Asian J. Chem.* **2010**, *22*, 539–545.
(44) Santos-Ebinuma, V. C.; Lopes, A. M.; Converti, A.; Pessoa, A.; Rangel-Yagui, C. de O. Behavior of Triton X-114 cloud point in the presence of inorganic electrolytes. *Fluid Phase Equilib.* **2013**, *360*, 435–438.
(45) Gu, T.; Galera-Gómez, P. A. Clouding of Triton X-114: The effect of added electrolytes on the cloud point of Triton X-114 in the presence of ionic surfactants. *Colloids Surfaces A Physicochem. Eng. Asp.* **1995**, *104*, 307–312.
(46) Taechangam, P.; Scamehorn, J. F.; Osuwan, S.; Rirksomboon, T. Effect of nonionic surfactant molecular structure on cloud point extraction of phenol from wastewater. *Colloids Surfaces A Physicochem. Eng. Asp.* **2009**, *347*, 200–209.
(47) Bordier, C. Phase separation of integral membrane proteins in Triton X-114 solution. *J. Biol. Chem.* **1981**, *256* , 1604–1607.
(48) Kamei, D. T.; King, J. A.; Wang, D. I. C.; Blankschtein, D. Separating lysozyme from bacteriophage P22 in two-phase aqueous micellar systems. *Biotechnol. Bioeng.* **2002**, *80*, 233–236.
(49) Jaramillo, P. M. D.; Gomes, H. A. R.; de Siqueira, F. G.; Homem-de-Mello, M.; Filho, E. X. F.; Magalhães, P. O. Liquid–liquid extraction of pectinase produced

by Aspergillus oryzae using aqueous two-phase micellar system. *Sep. Purif. Technol.* **2013**, *120*, 452–457.
(50) Mashayekhi, F.; Meyer, A. S.; Shiigi, S. A.; Nguyen, V.; Kamei, D. T. Concentration of mammalian genomic DNA using two-phase aqueous micellar systems. *Biotechnol. Bioeng.* **2009**, *102*, 1613–23.
(51) Jozala, A. F.; Lopes, A. M.; Mazzola, P. G.; Magalhães, P. O.; Penna, T. C. V.; Jr., A. P. Liquid–liquid extraction of commercial and biosynthesized nisin by aqueous two-phase micellar systems. *Enzyme Microb. Technol.* **2008**, *42*, 107–112.
(52) Santos, V. C.; Hasmann, F. A.; Converti, A.; Pessoa, A. Liquid–liquid extraction by mixed micellar systems: A new approach for clavulanic acid recovery from fermented broth. *Biochem. Eng. J.* **2011**, *56*, 75–83.
(53) Tong, A.; Wu, Y.; Tan, S.; Li, L.; Akama, Y.; Tanaka, S. Aqueous two-phase system of cationic and anionic surfactant mixture and its application to the extraction of porphyrins and metalloporphyrins. *Anal. Chim. Acta* **1998**, *369*, 11–16.
(54) Kamei, D. T.; Wang, D. I. C.; Blankschtein, D. Fundamental Investigation of Protein Partitioning in Two-Phase Aqueous Mixed (Nonionic/Ionic) Micellar Systems. *Langmuir* **2002**, *18*, 3047–3057.
(55) Bowers, J.; Butts, C. P.; Martin, P. J.; Vergara-Gutierrez, M. C.; Heenan, R. K. Aggregation Behavior of Aqueous Solutions of Ionic Liquids. *Langmuir* **2004**, *20*, 2191–2198.
(56) Wang, J.; Wang, H.; Zhang, S.; Zhang, H.; Zhao, Y. Conductivities, Volumes, Fluorescence, and Aggregation Behavior of Ionic Liquids [C4mim][BF4] and [Cnmim]Br (n = 4, 6, 8, 10, 12) in Aqueous Solutions. *J. Phys. Chem. B* **2007**, *111*, 6181–6188.
(57) Łuczak, J.; Jungnickel, C.; Joskowska, M.; Thöming, J.; Hupka, J. Thermodynamics of micellization of imidazolium ionic liquids in aqueous solutions. *J. Colloid Interface Sci.* **2009**, *336*, 111–116.
(58) Blesic, M.; Marques, M. H.; Plechkova, N. V; Seddon, K. R.; Rebelo, L. P. N.; Lopes, A. Self-aggregation of ionic liquids: micelle formation in aqueous solution. *Green Chem.* **2007**, *9*, 481–490.
(59) Miskolczy, Z.; Sebők-Nagy, K.; Biczók, L.; Göktürk, S. Aggregation and micelle formation of ionic liquids in aqueous solution. *Chem. Phys. Lett.* **2004**, *400*, 296–300.
(60) Comelles, F.; Ribosa, I.; González, J. J.; Garcia, M. T. Interaction of Nonionic Surfactants and Hydrophilic Ionic Liquids in Aqueous Solutions: Can Short Ionic Liquids Be More Than a Solvent? *Langmuir* **2012**, *28*, 14522–14530.
(61) Behera, K.; Pandey, S. Interaction between ionic liquid and zwitterionic surfactant: a comparative study of two ionic liquids with different anions. *J. Colloid Interface Sci.* **2009**, *331*, 196–205.
(62) Singh, K.; Marangoni, D. G.; Quinn, J. G.; Singer, R. D. Spontaneous vesicle formation with an ionic liquid amphiphile. *J. Colloid Interface Sci.* **2009**, *335*, 105–111.
(63) Smirnova, N. a; Vanin, A. a; Safonova, E. a; Pukinsky, I. B.; Anufrikov, Y. a; Makarov, A. L. Self-assembly in aqueous solutions of imidazolium ionic liquids and their mixtures with an anionic surfactant. *J. Colloid Interface Sci.* **2009**, *336*, 793–802.
(64) Chen, L. G.; Bermudez, H. Charge Screening between Anionic and Cationic Surfactants in Ionic Liquids. *Langmuir* **2013**, *29*, 2805–2808.

(65) Pramanik, R.; Sarkar, S.; Ghatak, C.; Rao, V. G.; Mandal, S.; Sarkar, N. Effects of 1-Butyl-3-methyl Imidazolium Tetrafluoroborate Ionic Liquid on Triton X-100 Aqueous Micelles: Solvent and Rotational Relaxation Studies. *J. Phys. Chem. B* **2011**, *115*, 6957–6963.
(66) Chen, L. G.; Bermudez, H. Solubility and Aggregation of Charged Surfactants in Ionic Liquids. *Langmuir* **2012**, *28*, 1157–1162.
(67) Ventura, S. P. M.; Santos, L. D. F.; Saraiva, J. A.; Coutinho, J. A. P. Ionic liquids microemulsions: the key to Candida antarctica lipase B superactivity. *Green Chem.* **2012**, *14*, 1620–1625.
(68) Hüttemann, M.; Pecina, P.; Rainbolt, M.; Sanderson, T. H.; Kagan, V. E.; Samavati, L.; Doan, J. W.; Lee, I. The multiple functions of cytochrome c and their regulation in life and death decisions of the mammalian cell: From respiration to apoptosis. *Mitochondrion* **2011**, *11*, 369–381.
(69) Lutic, D.; Coromelci-Pastravanu, C.; Cretescu, I.; Poulios, I.; Stan, C.-D. Photocatalytic Treatment of Rhodamine 6G in Wastewater Using Photoactive ZnO. *Int. J. Photoenergy* **2012**, *2012*, 1–8.
(70) Othman, N.; Yi, O. Z.; Zailani, S. N.; Zulkifli, E. Z.; Subramaniam, S. Extraction of Rhodamine 6G Dye from Liquid Waste Solution: Study on Emulsion Liquid Membrane Stability Performance and Recovery. *Sep. Sci. Technol.* **2013**, *48*, 1177–1183.
(71) Duran, C.; Ozdes, D.; Bulut, V. N.; Tufekci, M.; Soylak, M. Cloud-Point Extraction of Rhodamine 6G by Using Triton X-100 as the Non-Ionic Surfactant. *Journal of AOAC International*, *94*, 286–292.
(72) Blankschtein, D.; Thurston, G. M.; Benedek, G. B. Phenomenological theory of equilibrium thermodynamic properties and phase separation of micellar solutions. *J. Chem. Phys.* **1986**, *85*.
(73) Sharma, R.; Mahajan, S.; Mahajan, R. K. Surface adsorption and mixed micelle formation of surface active ionic liquid in cationic surfactants: Conductivity, surface tension, fluorescence and {NMR} studies. *Colloids Surfaces A Physicochem. Eng. Asp.* **2013**, *427*, 62–75.
(74) Kohno, Y.; Ohno, H. Temperature-responsive ionic liquid/water interfaces: relation between hydrophilicity of ions and dynamic phase change. *Phys. Chem. Chem. Phys.* **2012**, *14*, 5063–5070.
(75) Wang, X.; Liu, J.; Yu, L.; Jiao, J.; Wang, R.; Sun, L. Surface adsorption and micelle formation of imidazolium-based zwitterionic surface active ionic liquids in aqueous solution. *J. Colloid Interface Sci.* **2013**, *391*, 103–10.
(76) Qi, X.; Zhang, X.; Luo, G.; Han, C.; Liu, C.; Zhang, S. Mixing Behavior of Conventional Cationic Surfactants and Ionic Liquid Surfactant 1-Tetradecyl-3-methylimidazolium Bromide ([C14mim]Br) in Aqueous Medium. *J. Dispers. Sci. Technol.* **2012**, *34*, 125–133.
(77) Schott, H.; Royce, A. E.; Han, S. K. Effect of inorganic additives on solutions of nonionic surfactants: VII. Cloud point shift values of individual ions. *J. Colloid Interface Sci.* **1984**, *98*, 196–201.
(78) Zhang, Y.; Cremer, P. S. Interactions between macromolecules and ions: the Hofmeister series. *Curr. Opin. Chem. Biol.* **2006**, *10*, 658–663.
(79) Keilin, D.; Hartree, E. F. Purification and properties of cytochrome c. *Biochem. J.* **1945**, *39*, 289.
(80) ChemSpider – The free chemical database at www.chemspider.com. (Accessed on March 2014).

(81) Lu, Y.; Lu, W.; Wang, W.; Guo, Q.; Yang, Y. Thermodynamic studies of partitioning behavior of cytochrome c in ionic liquid-based aqueous two-phase system. *Talanta* **2011**, *85*, 1621–1626.
(82) Louros, C. L. S.; Cláudio, A. F. M.; Neves, C. M. S. S.; Freire, M. G.; Marrucho, I. M.; Pauly, J.; Coutinho, J. A. P. Extraction of Biomolecules Using Phosphonium-Based Ionic Liquids + K3PO4 Aqueous Biphasic Systems. *Int. J. Mol. Sci.* **2010**, *11*, 1777–1791.
(83) Ooi, C. W.; Tan, C. P.; Hii, S. L.; Ariff, A.; Ibrahim, S.; Ling, T. C. Primary recovery of lipase derived from Burkholderia sp. ST8 with aqueous micellar two-phase system. *Process Biochem.* **2011**, *46*, 1847–1852.
(84) Amid, M.; Abd Manap, M.; Shuhaimi, M. Purification of a novel protease enzyme from kesinai plant (Streblus asper) leaves using a surfactant–salt aqueous micellar two-phase system: a potential low cost source of enzyme and purification method. *Eur. Food Res. Technol.* **2013**, *237*, 601–608.
(85) Dua, R.; Shrivastava, S.; Shrivastava, S. L.; Srivastava, S. K. Green Chemistry and Environmental Technologies: A Review. *Middle-East J. Sci. Res.* **2012**, *11*, 846–855.
(86) Philippe, M.; Didillon, B.; Gilbert, L. Industrial commitment to green and sustainable chemistry: using renewable materials & developing eco-friendly processes and ingredients in cosmetics. *Green Chem.* **2012**, *14*, 952–956.
(87) S.J.Kulkarni; Maske, K. N.; Budre, M. P.; Mahajan, R. P. Extraction and purification of curcuminoids from Turmeric (curcuma longa L.). *Int. J. Pharmacol. Pharm. Technol.* **2012**, *1*, 81–84.
(88) Popuri, A. K.; Pagala, B. Extraction of Curcumin from Turmeric Roots. *Int. J. Innov. Res. Stud.* **2013**, *2*, 289–299.
(89) Revathy, S.; Elumalai, S.; Benny, M.; Antony, B. Isolation, Purification and Identification of Curcuminoids from Turmeric (Curcuma longa L.) by Column Chromatography. *J. Exp. Sci.* **2011**, *2*, 21–25.
(90) Stransky, C. E. Process for producing water and oil soluble curcumin coloring agents, 1979.
(91) Jurenka, J. S. Anti-inflammatory properties of curcumin, a major constituent of Curcuma longa: a review of preclinical and clinical research. *Altern. Med. Rev.* **2009**, *14*, 141–153.
(92) Esatbeyoglu, T.; Huebbe, P.; Ernst, I. M. A.; Chin, D.; Wagner, A. E.; Rimbach, G. Curcumin-From Molecule to Biological Function. *Angew. Chemie Int. Ed.* **2012**, *51*, 5308–5332.
(93) Wilken, R.; Veena, M. S.; Wang, M. B.; Srivatsan, E. S. Curcumin: A Review of Anti-Cancer Properties and Therapeutic Activity in Head & Neck Squamous Cell Carcinoma. *Mol. Cancer* **2011**, *10*, 12.
(94) Yallapu, M. M.; Jaggi, M.; Chauha, S. C. Curcumin Nanomedicine: A Road to Cancer Therapeutics. *Curr. Pharm. Des.* **2013**, *19*, 1994–2010.
(95) Ataie, A.; Sabetkasaei, M.; Haghparast, A.; Moghaddam, A. H.; Kazeminejad, B. Neuroprotective effects of the polyphenolic antioxidant agent, Curcumin, against homocysteine-induced cognitive impairment and oxidative stress in the rat. *Pharmacol. Biochem. Behav.* **2010**, *96*, 378–85.
(96) McCrate, O. A.; Zhou, X.; Cegelski, L. Curcumin as an amyloid-indicator dye in E. coli. *Chem. Commun.* **2013**, *49*, 4193–4195.
(97) Kerkeni, A.; Behary, N.; Perwuelz, A.; Gupta, D. Dyeing of woven polyester fabric with curcumin: effect of dye concentrations and surface pre-activation

using air atmospheric plasma and ultraviolet excimer treatment. *Color. Technol.* **2012**, *128*, 223–229.
(98) Kim, H.-J.; Kim, D.-J.; Karthick, S. N.; Hemalatha, K. V.; Raj, C. J.; Ok, S.; Choe, Y. Curcumin Dye Extracted from Curcuma longa L. Used as Sensitizers for Efficient Dye-Sensitized Solar Cells. *Int. J. Electrochem. Sci.* **2013**, *8*, 8320–8328.
(99) ChemSpider – The free chemical database at www.chemspider.com. (Accessed on 13th May 2014).
(100) Passos, H.; Sousa, A. C. A.; Pastorinho, M. R.; Nogueira, A. J. A.; Rebelo, L. P. N.; Coutinho, J. A. P.; Freire, M. G. Ionic-liquid-based aqueous biphasic systems for improved detection of bisphenol A in human fluids. *Anal. Methods* **2012**, *4*, 2664–2667.
(101) Weiss, R. A. How does HIV cause AIDS? *Science (80-.).* **1993**, *260*, 1273–1279.
(102) World Health Organization - Global Health Observatory- HIV/AIDS, accessed at http://www.who.int/gho/hiv/en/ on 9th April 2014.
(103) AIDS.gov - U.S. Government HIV/AIDS Information, accessed at http://aids.gov/hiv-aids-basics/just-diagnosed-with-hiv-aids/treatment-options/overview-of-hiv-treatments/ on 10th April 2014.
(104) Fung, H. B.; Stone, E. A.; Piacenti, F. J. Tenofovir disoproxil fumarate: A nucleotide reverse transcriptase inhibitor for the treatment of {HIV} infection. *Clin. Ther.* **2002**, *24*, 1515–1548.
(105) Kearney, B.; Flaherty, J.; Shah, J. Tenofovir Disoproxil Fumarate. *Clin. Pharmacokinet.* **2004**, *43*, 595–612.
(106) Palombo, M. S.; Singh, Y.; Sinko, P. J. Prodrug and conjugate drug delivery strategies for improving HIV/AIDS therapy. *J. Drug Deliv. Sci. Technol.* **2009**, *19*, 3–14.
(107) Shaw, J.-P.; Sueoka, C.; Oliyai, R.; Lee, W.; Arimilli, M.; Kim, C.; Cundy, K. Metabolism and Pharmacokinetics of Novel Oral Prodrugs of 9-[(R)-2-(phosphonomethoxy)propyl]adenine (PMPA) in Dogs. *Pharm. Res.* **1997**, *14*, 1824–1829.
(108) Delahunty, T.; Bushman, L.; Fletcher, C. V. Sensitive assay for determining plasma tenofovir concentrations by LC/MS/MS. *J. Chromatogr. B* **2006**, *830*, 6–12.
(109) Sentenac, S.; Fernandez, C.; Thuillier, A.; Lechat, P.; Aymard, G. Sensitive determination of tenofovir in human plasma samples using reversed-phase liquid chromatography. *J. Chromatogr. B* **2003**, *793*, 317–324.
(110) Kandagal, P. B.; Manjunatha, D. H.; Seetharamappa, J.; Kalanur, S. S. RP-HPLC Method for the Determination of Tenofovir in Pharmaceutical Formulations and Spiked Human Plasma. *Anal. Lett.* **2008**, *41*, 561–570.
(111) Rezk, N. L.; Crutchley, R. D.; Kashuba, A. D. M. Simultaneous quantification of emtricitabine and tenofovir in human plasma using high-performance liquid chromatography after solid phase extraction. *J. Chromatogr. B* **2005**, *822*, 201–208.
(112) Gomes, N. A.; Vaidya, V. V; Pudage, A.; Joshi, S. S.; Parekh, S. A. Liquid chromatography–tandem mass spectrometry (LC–MS/MS) method for simultaneous determination of tenofovir and emtricitabine in human plasma and its application to a bioequivalence study. *J. Pharm. Biomed. Anal.* **2008**, *48*, 918–926.
(113) Kromdijk, W.; Pereira, S. A.; Rosing, H.; Mulder, J. W.; Beijnen, J. H.; Huitema, A. D. R. Development and validation of an assay for the simultaneous

determination of zidovudine, abacavir, emtricitabine, lamivudine, tenofovir and ribavirin in human plasma using liquid chromatography–tandem mass spectrometry. *J. Chromatogr. B* **2013**, *919–920*, 43–51.
(114) Delahunty, T.; Bushman, L.; Robbins, B.; Fletcher, C. V. The simultaneous assay of tenofovir and emtricitabine in plasma using LC/MS/MS and isotopically labeled internal standards. *J. Chromatogr. B* **2009**, *877*, 1907–1914.
(115) Le Saux, T.; Chhun, S.; Rey, E.; Launay, O.; Weiss, L.; Viard, J.-P.; Pons, G.; Jullien, V. Quantification of seven nucleoside/nucleotide reverse transcriptase inhibitors in human plasma by high-performance liquid chromatography with tandem mass-spectrometry. *J. Chromatogr. B* **2008**, *865*, 81–90.
(116) Barkil, M. El; Gagnieu, M.-C.; Guitton, J. Relevance of a combined UV and single mass spectrometry detection for the determination of tenofovir in human plasma by HPLC in therapeutic drug monitoring. *J. Chromatogr. B* **2007**, *854*, 192–197.
(117) Jullien, V.; Tréluyer, J.-M.; Pons, G.; Rey, E. Determination of tenofovir in human plasma by high-performance liquid chromatography with spectrofluorimetric detection. *J. Chromatogr. B* **2003**, *785*, 377–381.
(118) Sparidans, R. W.; Crommentuyn, K. M. L.; Schellens, J. H. M.; Beijnen, J. H. Liquid chromatographic assay for the antiviral nucleotide analogue tenofovir in plasma using derivatization with chloroacetaldehyde. *J. Chromatogr. B* **2003**, *791*, 227–233.
(119) Sosa Ferrera, Z.; Padrón Sanz, C.; Mahugo Santana, C.; Santana Rodríguez, J. J. The use of micellar systems in the extraction and pre-concentration of organic pollutants in environmental samples. *TrAC Trends Anal. Chem.* **2004**, *23*, 469–479.
(120) Rezk, N. L.; Tidwell, R. R.; Kashuba, A. D. M. Simultaneous determination of six HIV nucleoside analogue reverse transcriptase inhibitors and nevirapine by liquid chromatography with ultraviolet absorbance detection. *J. Chromatogr. B* **2003**, *791*, 137–147.
(121) Xie, X.; Wang, Y.; Han, J.; Yan, Y. Extraction mechanism of sulfamethoxazole in water samples using aqueous two-phase systems of poly(propylene glycol) and salt. *Anal. Chim. Acta* **2011**, *687*, 61–66.
(122) He, C.; Li, S.; Liu, H.; Li, K.; Liu, F. Extraction of testosterone and epitestosterone in human urine using aqueous two-phase systems of ionic liquid and salt. *J. Chromatogr. A* **2005**, *1082*, 143–149.
(123) Du, Z.; Yu, Y.-L.; Wang, J.-H. Extraction of Proteins from Biological Fluids by Use of an Ionic Liquid/Aqueous Two-Phase System. *Chem. – A Eur. J.* **2007**, *13*, 2130–2137.
(124) Freire, M. G.; Neves, C. M. S. S.; Marrucho, I. M.; Canongia Lopes, J. N.; Rebelo, L. P. N.; Coutinho, J. A. P. High-performance extraction of alkaloids using aqueous two-phase systems with ionic liquids. *Green Chem.* **2010**, *12*, 1715–1718.
(125) Vicente, F. A.; Malpiedi, L. P.; Silva, F. A. e; Jr., A. P.; Coutinho, J. A. P.; Ventura, S. P. M. Design of novel aqueous micellar two-phase systems using ionic liquids as co-surfactants for the selective extraction of (bio)molecules. *Sep. Purif. Technol.* **2014**.
(126) Gomes, G. A.; Azevedo, A. M.; Aires-Barros, M. R.; Prazeres, D. M. F. Purification of plasmid DNA with aqueous two phase systems of PEG 600 and sodium citrate/ammonium sulfate. *Sep. Purif. Technol.* **2009**, *65*, 22–30.

(127) AIDSinfo, a service of the U.S. Department of Health and Human Services at http://aidsinfo.nih.gov/drugs/290/tenofovir-disoproxil-fumarate/0/professional (Accessed at 22nd May 2014).
(128) Pourreza, N.; Rastegarzadeh, S.; Larki, A. Determination of Allura red in food samples after cloud point extraction using mixed micelles. *Food Chem.* **2011**, *126*, 1465–1469.
(129) Rito-Palomares, M.; Hernandez, M. Influence of system and process parameters on partitioning of cheese whey proteins in aqueous two-phase systems. *J. Chromatogr. B Biomed. Sci. Appl.* **1998**, *711*, 81–90.
(130) Da Silva, C. A. S.; Coimbra, J. S. R.; Rojas, E. E. G.; Teixeira, J. A. C. Partitioning of glycomacropeptide in aqueous two-phase systems. *Process Biochem.* **2009**, *44*, 1213–1216.
(131) Zhang, S.; Wang, J.; Lu, X.; Zhou, Q. *Structures and Interactions of Ionic Liquids*; Structure and Bonding; Springer London, Limited, 2013.
(132) Liu, Y.; Wu, Z.; Zhang, Y.; Yuan, H. Partitioning of biomolecules in aqueous two-phase systems of polyethylene glycol and nonionic surfactant. *Biochem. Eng. J.* **2012**, *69*, 93–99.
(133) ZHAO, X.-Y.; QU, F.; DONG, M.; CHEN, F.; LUO, A.-Q.; ZHANG, J.-H. Separation of Proteins by Aqueous Two-phase Extraction System Combined with Liquid Chromatography. *Chinese J. Anal. Chem.* **2012**, *40*, 38–42.
(134) Li, S.; He, C.; Liu, H.; Li, K.; Liu, F. Ionic liquid-based aqueous two-phase system, a sample pretreatment procedure prior to high-performance liquid chromatography of opium alkaloids. *J. Chromatogr. B* **2005**, *826*, 58–62.
(135) Sirimanne, S. R.; Barr, J. R.; Patterson, D. G.; Ma, L. Quantification of Polycyclic Aromatic Hydrocarbons and Polychlorinated Dibenzo-p-dioxins in Human Serum by Combined Micelle-Mediated Extraction (Cloud-Point Extraction) and HPLC. *Anal. Chem.* **1996**, *68*, 1556–1560.
(136) Bhatt, D.; Maheria, K.; Parikh, J. Mixed system of ionic liquid and non-ionic surfactants in aqueous media: Surface and thermodynamic properties. *J. Chem. Thermodyn.* **2014**, *74*, 184–192.
(137) Pal, A.; Chaudhary, S. Ionic liquids effect on critical micelle concentration of SDS: Conductivity, fluorescence and NMR studies. *Fluid Phase Equilib.* **2014**, *372*, 100–104.
(138) TOCCHINI, L.; MERCADANTE, A. Z. Extraction and determination of bixin and norbixin in annatto spice ("Colorifico"). *Food Science and Technology (Campinas)*, 2001, *21*, 310–313.
(139) Costa, C. L. S. da; Chaves, M. H. Extraction of pigments from seeds of Bixa orellana L.: an alternative for experimental courses in organic chemistry. *Química Nova*, 2005, *28*, 149–152.
(140) Barroso, R.; da Rocha, P.; Emmi, D.; de Nazare, R. R. Bacterial plaque evidencing composition based on natural colorants, 2004.
(141) Barcelos, G. R. M.; Grotto, D.; Serpeloni, J. M.; Aissa, A. F.; Antunes, L. M. G.; Knasmüller, S.; Barbosa, F. Bixin and norbixin protect against DNA-damage and alterations of redox status induced by methylmercury exposure in vivo. *Environ. Mol. Mutagen.* **2012**, *53*, 535–541.
(142) Malpiedi, L. P.; Nerli, B. B.; Abdalla, D. S. P.; Pessoa, A. Assessment of the effect of triton X-114 on the physicochemical properties of an antibody fragment. *Biotechnol. Prog.* **2014**, n/a–n/a.
(143) Malpiedi, L. P.; Nerli, B. B.; Abdala, D. S.; Pessôa-Filho, P.; Jr, A. P. Aqueous micellar systems containing Triton X-114 and Pichia pastoris fermentation

supernatant: a novel alternative for single chain-antibody fragment purification. *Sep. Purif. Technol.* **2014**, *accepted*,.

(144) Pavan, R.; Jain, S.; Shraddha; Kumar, A. Properties and Therapeutic Applications of Bromelain: a Review. *Biotechnol. Res. Int.* **2012**, *2012*, 1–6.